UNIVERSITY OF CAPE COAST

MORPHOLOGICAL FEATURES OF THE WHITE VOLTA RIVER: AN EVALUATION OF THEMATIC ACCURACY

BENEDICT TETTEH KOJO NARTEY

2017

UNIVERSITY OF CAPE COAST

MORPHOLOGICAL FEATURES OF THE WHITE VOLTA RIVER: AN EVALUATION OF THEMATIC ACCURACY

BY

BENEDICT TETTEH KOJO NARTEY

Thesis submitted to the Department of Geography and Regional Planning of the Faculty of Social Sciences, College of Humanities and Legal Studies, University of Cape Coast, in partial fulfilment of the requirements for the award of Master of Philosophy degree in Geography and Regional Planning

JULY 2017

DECLARATION

Candidate's Declaration

I hereby declare that this thesis is the result of my own original research and that no part of it has been presented for another degree in this university or elsewhere.

Candidate's Signature……Date……

Name: Benedict Tetteh Kojo Nartey

Supervisor's Declaration

We hereby declare that the preparation and presentation of the thesis were supervised in accordance with the guidelines on supervision of thesis laid down by the University of Cape Coast.

Principal Supervisor's Signature……. Date……

Name: Dr. Benjamin Kofi Nyarko

Co- Supervisor's Signature……. Date……

Name: Prof Laud A. Dei

ABSTRACT

Rivers are natural forces that continue to shape the surface of the earth and also play an important role in supporting life. They serve as part of the earth's interconnected circulatory system. This system acts on the rivers to alter topography and shape of river basins and nearby landmasses which influence river currents. Earth observation tools have developed over the years with enhanced and advanced technological input to also observe such changes. The White Volta has been affected by various factors both natural and anthropogenic activities causing some changes within its basin. But methods to extract such features for observation are now numerous. In order to know the effective method in semi-automatic riverine feature extraction, the study compared the pixel based, object based and the decision tree image classification methods conducted on remotely sensed data of the White Volta. The Landsat 8 OLI image data was used for the classification in ENVI software. The Maximum Likelihood Classification (M LC) had a kappa coefficient of 0.9492, the Decision Tree Classification (DTC) had a kappa of 0.9491 and the Object Based Classification (OBC) had a kappa index of agreement of 0.9505. the total accuracies were what differentiated them all vastly with the MLC, DTC and the OBC attaining 98.48%, 99.9% and 97.37% respectfully. The study however found the OBC to be a preferred choice because it was able to overcome the deficiencies of the other two methods and still attain a competitive accuracy level. The study therefore recommended the OBC for the choicest in the event that there was the need for a choice but also acknowledged the efficiency of the remaining two methods.

KEYWORDS

Decision Tree

Extraction

Morphometric Analysis

Object-Based

Pixel-Based

White Volta

ACKNOWLEDGEMENT

Writing this thesis wouldn't have been possible without the effort of some people who did their best to make this a success. Firstly, I express my immense gratitude to my supervisors' Dr B. K. Nyarko and Professor L. A. Dei for their unwavering support in making this a success. For their patience, trust and believe in me to accomplish this work successfully.

I also want to appreciate my parents Mr. Sampson Nartey and Mrs. Grace Nartey for their greatest support in these times and for the financial support to bring me this far. Their prayers and encouragement was very helpful to me.

Finally, I show appreciation to Prof K. Barima Antwi (academic counsellor), Mr. E. A. Mensah, Mr Kinsley Osei, Mr Osman Adams, Mr Christian Kwesi Owusu, Mr Richard Adade, Mr Prince Kwame Odame, my course mates and all who helped in diverse ways to make this thesis a success and above all, my appreciation is to Almighty God who gave me good health, wisdom and strength to come this far.

DEDICATION

To my brothers, Emma and Steve

TABLE OF CONTENTS

LIST OF TABLES

LIST OF FIGURES

CHAPTER ONE

INTRODUCTION

Background to the Study

Rivers continue to shape and carve into the surface of the earth and also play a major role in supporting life. For instance, rivers supply humans with water for domestic and commercial uses (such as irrigate farmlands, power cities with hydroelectricity). They serve as part of the earth's interconnected circulatory system. This system powered by the sun (solar energy) acts on the rivers and other water bodies thereby creating differences in water density and forces leading to shaping of river basins and nearby landmasses. These processes and physical characteristics of the river system influence its size, shape, speed, and direction of river currents (Cowan, 2013).

The entire course of a river experience two primary processes that are erosion and deposition (Dey, 2014). Erosional process along a river is one of the most powerful activities that it undertakes. Though rivers are among the most powerful forces that act to shape the surface of the earth, their works are visible in their appearance in the form of surface features (Hecher, Filippi, Guneralp and Paulus, 2012). The nature of river features has been of concern to geomorphologist, geologists and engineers because the dynamics of river channels have practical implications for land use, sediment budget, and navigation (Howard & Knutson, 1984). Understanding the nature of river features and predicting conditions leading

to their formation should be discussed rationally from the spatial and temporal perspective (Slingerland & Smith, 1998).

The spatio-temporal dynamics of any river system is characterised by recurrent river planform patterns, repeated with little variation irrespective of their magnitude and geometry in different settings (Hans-Henrik, 1996)

Information about the spatio-temporal dynamics of river planform is a vital input for most developmental projects, planning, resource exploitation among others on local, regional and global scales. It's been noted that remote sensing is by far the cost effective and efficient method that can be used to gather data about the dynamics of a river system (Minjie, et al., 2008). Extracting information from remotely sensed imagery depends on the complexity of the classification methods, landscape, the spatial and spectral resolution of the imagery.

According to Weih and Riggan, Jr. (2010) researchers have adopted different classification methods to identify the morphology of any physical feature from satellite imagery. Therefore image classification methods can be subdivided into supervised and unsupervised, and object-oriented, per-pixel, sub-pixel and per-field classifications.

Several classification techniques employed (spatial and spectral) the pixel as the core unit of analysis. Broad categories of classification techniques have been developed for identification of elements or features from satellite images (Minjie, et al., 2008). Examples are unsupervised (i.e. k-means and Iterative Self-Organising Data Analysis Technique (ISODATA)), supervised (i.e. maximum likelihood, decision tree, support vector machine,), and hybrid classification (i.e. semi-

supervised and fusion of supervised and unsupervised learning) (Alajlan et al., 2012). Therefore, the ability to process and analyse imagery from remote sensors using these classification methods to extract data and information about the river systems allow researchers and policy makers monitor occurrences on the earth surface feature and take decisions that are appropriate and timely.

Problem Statement

In the past years, researchers and technocrats have applied different methods and techniques to extract data from remotely sensed images, to enable them understand water resource systems in Ghana. For instance, different extraction and classification methods such as automated and semi-automated have been used over satellite imagery for riverine wetland thematic mapping and morphometric analysis of river system and their characteristics (Pisal, Yadav, & Chavan, 2013; Hecher et al, 2012). However, using these automated and semi-automated methods of extraction on images is often problematic owing to the vast spectral differences within one class (Myint, Gober, Brazel, Grossman-Clarke & Weng, 2011).

The nature and planform of the White Volta has been affected by different hydrological events (Water Resource Commission, 2008). Present processes and events such as climatic variations, land use/land cover changes, human activities, flood occurrences and sediment load, with different matrix of relationships are continually playing important roles in shaping the planform of the riverine system (WRC). These processes, have led to the formation of riverine features that need to

be identified, extracted and documented. Knowledge about these features within the White Volta is of tremendous benefit to geomorphologists, engineers and physical geographers for planning, formulating policies and decision making. Inadequate studies have been conducted to discover them and there is no documentation about them.

To delineate or extract riverine features, researchers have identified the use of satellite remote sensing as a source of data with improved spatial resolution that provides large area coverage that can aid in deriving riverine features.

A variety of methods to delineate rivers have been used with varying success (Davranche, Lefebvre & Poulin, 2010), less attention has been given to the applicability of such methods across rivers in Ghana. These studies also select methods based on recommendations of successful trials without comparison to specific features and appropriate methods. Hence, to verify how accurate semi-automatic method can be used to extract riverine feature from Landsat images, the study compared the pixel based (PBC), object based (OBC), the decision tree (DTC) and the spectral angle mapper (SAM) image classification methods conducted on remotely sensed data of the White Volta.

Research Questions

1. What riverine features can be extracted from the images with each classification method (PBC, OBC, DTC and SAM)?
2. What is the accuracy level of the various classification methods in extracting the riverine features along the White Volta?

3. What morphometric parameters can be derived based on the extracted output?

Main Objective

The main objective of the study is to extract morphological features of White Volta River, using medium resolution satellite imagery.

Specific Objectives

The specific objectives are to

1. Extract riverine morphological features in the catchment area using different classification method (PBC, OBC, DTC and SAM).
2. Assess the accuracy of the various classification methods in extracting the riverine features along the White Volta.
3. Compare morphometric analysis based on the output of each extraction method.

Significance of the study

Remote sensing and its application is gaining grounds in the Ghanaian contest and can be fully utilised to the benefits of many institutions that are yet to realise its potential. The study is, therefore, seeking to provide adequate assessment information that can be useful in the selection of the most efficient method for classifying images to monitor and protect the water bodies. The optimum method can aid in tracking and protecting the White Volta basin as a major tributary that

feeds into the Volta lake for the production of electricity mainly, as well as a source of living for communities along its bank and even transportation in some cases.

The development of thematic maps will also be a valuable asset for developmental projects for both the government and the private sector. These maps can serve as a base map for the development of the basin for natural resource preservation and recreation.

The ability to select the appropriate method to extract the features in the northern part of Ghana will ensure proper allocation of resources for resilience in harsh weather conditions.

The study will also unveil to satellite image users the method that is most reliable for water drainage feature extraction and classification in further research. Hence, creating the platform for the development of new models that will assist stakeholders in the formulation of effective strategies and in the development of suitable programs for poverty alleviation and food security in the surrounding communities. A good algorithm analysis will attract NGOs and international bodies like the UN, WHO among others to develop sustainable ideas to achieve the sustainable goals.

Organisation of the study

The introductory chapter of this thesis presented the background information of the study, statement of the research problem, research questions, research objectives, significance or rationale of the study and organisation of the

study. The chapter also delved into the discussion of the research problem and give the dimension of the problem.

Chapter Two gave a thorough review of the published literature covering the concepts and variables that were considered in this research. Related and relevant materials included relevant books on pixel based, object oriented and decision tree analysis in river and built up areas, published reports and articles on image classification analysis and techniques, newspapers and other internet sources that were relevant to the study.

Chapter Three discussed the methodology that were used in the study. It also introduced the study design that was adopted, study setting and target areas that were used for the research. The latter part of the chapter comprised the sources of data for the study, equipment and gadget for data collection and procedures for both quantitative data and data analysis techniques.

Chapter Four discussed the result and analysis of the study. In this chapter, three main areas would be covered. These areas were the derivation of thematic maps of the basin under the various lens of classification, assessing the accuracy levels of the methods and the morphometric analysis of the drainage area.

Chapter Five summarised the findings of the research; gave possible recommendations if any and conclusion. Then finally, the chapter summed up the whole study on the comparison of the three algorithms on the White Volta. The summary of the study comprised, the objectives of the study, major findings, conclusion from findings and recommendations to aid in assessing an accurate method for image classification

CHAPTER TWO

REVIEW OF RELATED LITERATURE

EXTRACTING MORPHOLOGICAL FEATURES IN RIVERS

Introduction

This chapter explains the literature related to this work and review other relevant literature that would inform the trends of the study. It involves the thoughts, ideas, perceptions and theories that have informed this study.

Riverine System

Several significant freshwater resources to man include rivers. In the past, the development of several communities had been mostly attributed to the availability and distribution of freshwaters and its resources contained in riverine systems (Meybeck, et al. 2000). A river is a network of complex systems of running water draining channels on the surface of the earth and are termed as river basins or watersheds when they all connect to the main channel. They are the most active agents of change among geomorphic forms. Evidence from several sources demonstrates that river channels are continually undergoing changes of position, shape, dimensions, and pattern (Richardson, Simon & Lagasse, 2001). The characteristics of streams, within the total basin system, are related to some features. These features often include the size, form and geological features of the

basin and the climatic conditions which influence the quantities of water to be drained by the river network.

Rivers may be classified using the type of flow regime and magnitude of discharge. Thus, flow categories may be dependent on significant changes by natural impoundments, lakes, dams, or water storage. Flow features may also be varied by canalisation, water demands for irrigation or other water supply needs, or by variety in flood characteristics due to modifications of the soil infiltration as a product of farming and urbanisation (Chapman, 1996).

Planform Formation Processes

The river channel is often described as being in a state of constant wriggle between the erosive potential the stream carries and the friction it encounters with the valley floor. The erosive and frictional forces contribute to the formation of these river planforms.

Erosion

River waters carry out two processes which are erosion and corrosion (Matsuda, 2004). Erosion occurs when the energy of running water removes sediments or scours the channel and remove sediments from the river bed. Erosion that deepens the channel is referred to as erosional downcutting or vertical erosion while lateral erosion refers to the broadening of the channel. The vertical erosion can result in the formation of a canyon. Continuous lateral erosion results in a river with a broad river bed (Matsuda).

The controlling factors in the formation of a river and a stream are both complex but interrelated. They are the amount and rate of supply of water and sediment into stream systems, catchment geology, and the type and extent of vegetation in the watershed. The alteration of these factors over time results in a corresponding change in the river systems by altering their shape, form and or location. The rate of change in steady streams are often slow and unnoticeable (Queensland, 2015). The Queensland Government in 2006 outlined a number of factors as catalysts for accelerated river erosion and they are, 1) stream bed lowering or infill, 2) inundation of bank soils followed by rapid drops in flow after flooding, 3) saturation of banks from off-stream sources, 4) redirection and acceleration of flow around infrastructure, obstructions, debris or vegetation within the stream channel, 5) removal or disturbance of protective vegetation from stream banks as a result of trees falling or through poorly managed stock grazing, clearing or fire 6) bank soil characteristics such as poor drainage or seams of readily erodible material within the bank profile, 7) wave action generated by wind or boat wash, 8) excessive or inappropriate sand and gravel extraction, 9) intense rainfall events (e.g. cyclones). These catalysts also influence the shapes and nature of river planforms.

In the understanding of erosion, Couture (2008) explained that erosion is a natural process which continuous unabated. Therefore, the type of soil, the slope, precipitation and velocity affect the rate of erosion. He also purported that erosion can be slowed but not stopped (Couture). River systems are dynamic systems that often balance water flow and sediment transport, hence, the river's energy tries to balance the size and volume of sediment carried by the river by way of its carrying

capacity. When rivers are altered by natural or anthropogenic factors, the rivers readjust to reach an equilibrium. The adjustment may affect the dimension, profile or the pattern of the river. The figure below shows the channel evolutionary model in the strive to achieve balance in a river channel and was adopted by Couture in 2008.

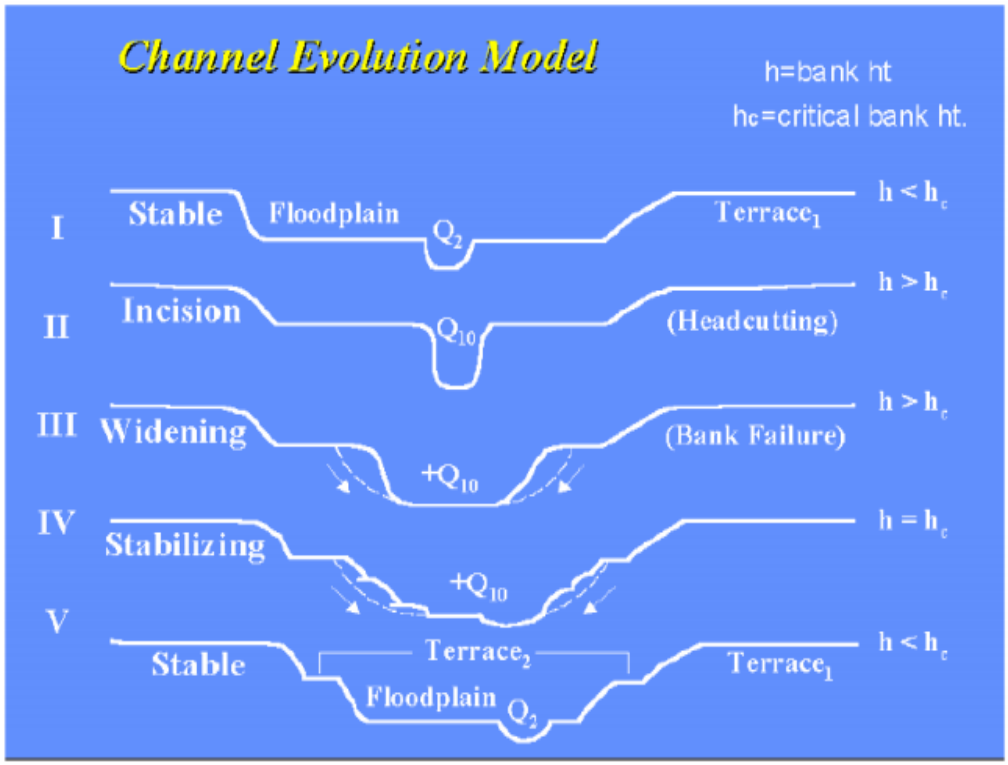

Figure 1: Channel Evolution Model

Source: Couture, 2008.

The model is an approach to understanding the fluvial system which are constantly changing and evolving, with no exception to the White Volta River. Collison (2016) explained that this constant change and evolution is an attempt to reach equilibrium. Hence he explained that a stable fluvial system is well vegetated, frequently interacts with its floodplains and the sediment is suspended. Inferring from his model, a river system continues to erode, thereby changing basin system

planforms till an equilibrium state is achieved. Therefore, channel evolution model helps to classify the current stage of the fluvial system to help in the prediction of how the system will evolve.

River banks can be eroded by two (2) processes which are bank scour and mass failure. Bank scour is the direct removal of bank material by the action of flowing water and the sediment it carries. Therefore, the flow rate is a key factor in the morphology of the river. The mass failure refers to the bank of rivers which slides or fall into the river. It refers to the total failure of a section of the river bank causing it to slide or topple into the river (Couture, 2008).

Sediment transportation

The transportation of materials in rivers begins after friction has been overcome. The reason being that river channel walls are not perfectly smooth. This channel roughness increases friction between the water and the channel, and makes the water flow more slowly than it otherwise would. In very few channels in which the water flow is smooth, some obstacles on the river bed cause swirling vortices to form. In most rivers, the water flow is turbulent (Reineck & Singh, 2012). This means although the primary flow is down the channel, within this channel the water flows in chaotic swirls and eddies (secondary flow) which come and go unpredictably. This turbulence helps the river to lift heavier objects off the river bed and transport them downstream. When the velocity profile of a river is plotted, that is a curve showing how the flow velocity varies with depth (depth = distance below the surface or the height above the river bed) then two main types of the velocity profile, each corresponding to a different flow regime can be drawn.

Reineck and Singh (2012) explained that the first type is the laminar flow regime, which is rare in natural rivers, but can occur when the river channel is smooth and straight and maximum flow velocity is low and may occur especially in the lower course of a river. In this case, the water flows effortlessly in sheets parallel to the river bed. Water at the surface has higher velocity than water close to the river bed, where flow is slowed by friction with the river bed. The second type is the turbulent flow regime, which occurs in complex winding channels and rivers with riffle and pool sequences and especially in fast flowing water. This is the most common type of flow regime. Rivers no longer flow in calm sheets, but swirls about in chaotic eddies that are unpredictable (Reineck & Singh).

Land use is a key geophysical characteristic that affects the amount of sediment transported within watersheds as a function of precipitation and runoff. Land use changes influence the permeability of land surfaces, infiltration rates of the soil, and amount of surface features that can disrupt flow. Abungba (2013) in his study of the White Volta River, revealed that watershed with steep slopes, low permeability, and few features obstructing the flow will tend to have high discharge rates of runoff into streams having a significant effect on streamflow. Land use change in such areas has been mainly the conversion of natural lands like forest and grassland, into agricultural lands and pastures. Conversion to agricultural lands and pastures is one of the largest and most historic land use change with some eco-hydrological consequences. The disruption of soils and reduction of plant cover increases the flow of runoff and movement of sediments from the landscape into fluvial systems. This effect is exacerbated if land with steep slopes and easily

erodible soils are cultivated and is also a function of the type of agriculture practised (Abungba).

Water with higher velocity has more carrying capacity for sediment load transportation. But there are three different processes in the transportation of sediment load. They are corrosion, suspension and traction. Corrosion involves the process in which stream water scrape rocks till it brings them invisibly into solution. Grinded sediments as clay, silt and fine sand are transported in the water or on the water surface without contact with the river bed. This transportation process is called suspension. The materials being carried in suspension are known as suspended loads which often create turbidity of stream water. The gravels having larger diameter are dragged or rolls, while sand hops or bounce off the river bed. These processes are called traction. Sediment load carried by traction is known as bed load (Matsuda, 2004).

River Features

The old age stage of a river has high volume and large discharge. The river channel is deep and has a broad riverbed. The flood plain is generally flat and the velocity at this stage of the river is low. Hence deposition is dominant, which result in the formation of features including those elaborated below.

Meanders

Numerous studies have suggested hypotheses to explain the origin of meandering, namely Coriolis force resulting from earth rotation, transverse flow oscillations caused by local flow disturbances, secondary flow, turbulence, wave

motion, bank erosion and bar formation, energy dissipation and minimum variance. Hence, they are grouped under the following broad categories; a) regime approach, b) minimum stream power, c) statistical theory and spectral analysis, d) secondary currents and e) stability analysis. Among these, the best explanation so far includes local disturbance, earth rotation, excessive energy and hydrodynamic stability, which all contribute to stability analysis (Julien, 1985: Lazarus & Constantine, 2013).

Hans-Henrik (1996) explained that meandering is the product of two opposing processes, linked by multiple feedback that is partially under local geometrical control: lateral migration which acts to increase sinuosity, whereas cutoffs (forms oxbow lakes) act to decrease sinuosity. Lateral migration results from bend erosion and deposition. Cutoffs arise from a local geometry (Kinoshita shape), which is created by the lateral migration process (Hans-Henrik).

Meandering rivers (sinuosity of greater than 1.5) are chains of turns with alternating curvatures connected at the points of inflection or by short straight crossings and have a calmly gentle slope. Naturally, meandering rivers are relatively unstable owing to predominant bank erosion downstream of concave banks. Deeper flows are prevalent in the bends and increased velocities along the outer concave banks. The flow depth at crossings is relatively shallow compared to that at bends. Meandering rivers tend to migrate gradually and hence sinuosity tends to increase. Eventually, the channel forms almost a closed loop and the meander gets often cut off during a flood. Meandering can be articulated to result of streambed instability, especially instability on the banks (Dey, 2014)

The flow and sediment transport are controlled by the riverbed nature, which in turn enhance changes in the riverbed. Thus, they are interdependent, and complement each other. The features of rivers are related to the gradient of the terrain that is from extremely steep mountainous torrents to steep rivers at the foot-hills and rivers in the plains. Therefore, a river could be regarded as it consisting of upper, middle, and lower reaches which correspond to erosion, regime and aggradations states, respectively. In the upper reach, the sediment transport capacity by the river flow is generally greater than the sediment being transported, leading to erosion of the streambed. In middle reach, the sediment transport rate is less than the transport capacity by the river due to gradual riverbed armouring followed by a long-term bed-sorting process. Thus, the river reaches a state of quiescent erosion or so-called regime. In lower reach, aggradations occur because of substantial decrease in transport capacity with decrease in valley slope (Dey, 2014).

Straight rivers have minimal sinuosity of less than 1.1. The curvature or meander usually measured by the length of the stream divided by the valley distance (straight line) between the end points of the curve is known as sinuosity (Harman, et al., 2013). In the case of a river (which is the focus of this study), it is the ratio of the actual river length to the down-valley length (bird flight length).

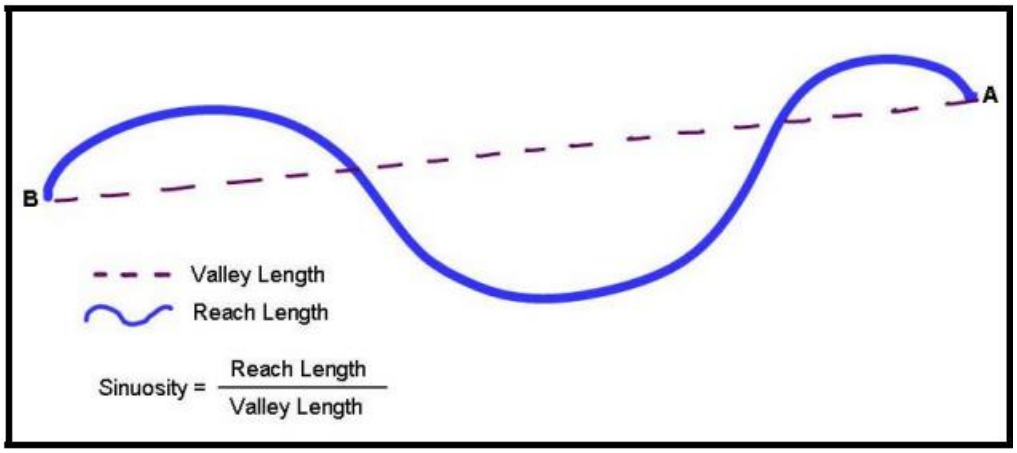

Figure 2: Figure showing the definition of sinuosity.

Source: Lohani (2008)

The sinuosity's minimum values mean unity for a perfectly straight river at the bank full conditions. Usually, rivers, as simple straight open channels, exist only over short reaches while long, straight rivers seldom occur in nature. At low flow stages, alluvial bars exist on either side of the stream. The thalweg may wind in a sinuous route along the bars, even though the channel is straight. The thalweg may move with alternate bars as they migrate downstream (Dey, 2014).

Hence, it is relevant to elaborate that the rivers with a sinuosity of less than 1.1 is described as straight, those between 1.1 and 1.5 are sinuous, and meandering rivers have a sinuosity of greater than 1.5. Therefore, sinuous rivers are the transition between straight and meandering rivers. Although these descriptions are commonly used by physical geographers, they are somewhat arbitrary, since they are not based on any physical differences. Further, there is a tendency for the thalweg to swing from side to side along the rivers. This is observed even in straight rivers and is often associated with the development of riffles, pools, and alternate bars (Dey, 2014).

Braided rivers are wide and shallow and divided to branches by a number of semi stable or unstable bars or islands. More specifically, braided river can be defined as one that consist of a network of small channels separated by small alluvial bars and frequently temporary islands. They have a braided look at the low flow stages with exposed bars, but all or some of the bars are submerged during the high flow stages because of increase in water volume. However, in most of the occasions, the branching is such that one is the main stream and the others are subsidiary channels. The main stream is relatively stable, but it can change its route under some flow and sediment transport conditions, while the subsidiary channels are quite unstable and often change during floods (Dey, 2014).

Meandering river features

Meandering rivers have produced features that exist as a result of river actions throughout evolution of river processes. Therefore, for the purpose of the study, river features formed along meandering rivers will be discussed.

Lakes

These are crescent or u-shaped waterbodies lying along winding rivers. They are formed from the continuous eroding of neighbouring river bends that eventually join cutting away the bend in the process. Hecher et al (2012) explained that the formation of an oxbow lake is either by lateral erosion or the result of flood. Hence the remnant meander loop is detached from the new straightened river course by the deposited sediments, creating the oxbow lake.

Figure 3:The oxbow lakes of the Nowitna River, Alaska

Source: Kurmis (2002)

Scars

Scars are oxbow lakes that have been filled with sediments. Hecher et al. (2012) looked at two types of deposition in the scars. He identified one as the heterolithic/active filling, which is predominantly sand representing a mixture of suspended and bed load. And the second as the passive filling, also dominated by lacustrine mud, suspended load and overbank fines. These are achieved with the aid of ephemeral streams between the scars and other water bodies.

Figure 4: Rio Negro Meander Scars, Argentina

Source: NASA Astrounaut Photograph (2010)

Sandbars

Sandbars also called point bars are meander river features characterised by continuous deposition of sediments along the meander loop of a river till the loop is cut off to form an oxbow lake. The deposition takes place on the inside of the river bend. Because they are slightly higher than the water level and have a gentle slope, they are likely to be overtaken by floods.

Relic Channels

These are formerly active river channels that have been deserted as a result of lateral river migration. Relic channels are similar to scars because they are depressions in the landscape that may include water.

Immoor (2006) identifies that old age rivers actually have several distinguishing features to exhibit than the youthful and mature rivers show. He

outlines a number of them some of which are relevant to this study. Like other researchers, Immoor identifies that old age rivers are wider than they are deep and have a very broad U-shaped valley owing to the extensive lateral erosion. It has a low velocity which makes it capable of moving small-sized sediments, i.e. silts and clays. The river at this stage is able to carry small sediments giving it a muddy look. Also dissolved salts and ions are carried in a solution. Furthermore, the general planform within which the river is located is flatter and has less steep slope. The hilly areas that exist are further away from the river channel separated by a wide floodplain which flanks the river. The old age river has curvy S-shaped meanders in abundance and this is a major feature. When the meanders are cut off from the main stream due to extensive erosion and deposition, they form oxbow lakes within the floodplain. Because it cut off from the main stream, it has no water supply to replenish those that would be lost. The lake would eventually dry up leaving what is referred to as a Meander scar (Immoor).

Channel morphology

According to Selander (2004), the morphology of a channel is mostly governed by a number of drivers including tectonic processes, climate/hydrologic regime and the changes therein, and local lithology which influence the river system over a period of time. In expatiating, he articulated that the tectonic uplift or subsidence of a catchment will result in a change in base level which will result in either a wave of incision propagating upstream (uplift, base level fall) (Whipple, 2004) or aggradation (subsidence, base level rise) as the channel adjusts. This is further illustrated in figure 2 below.

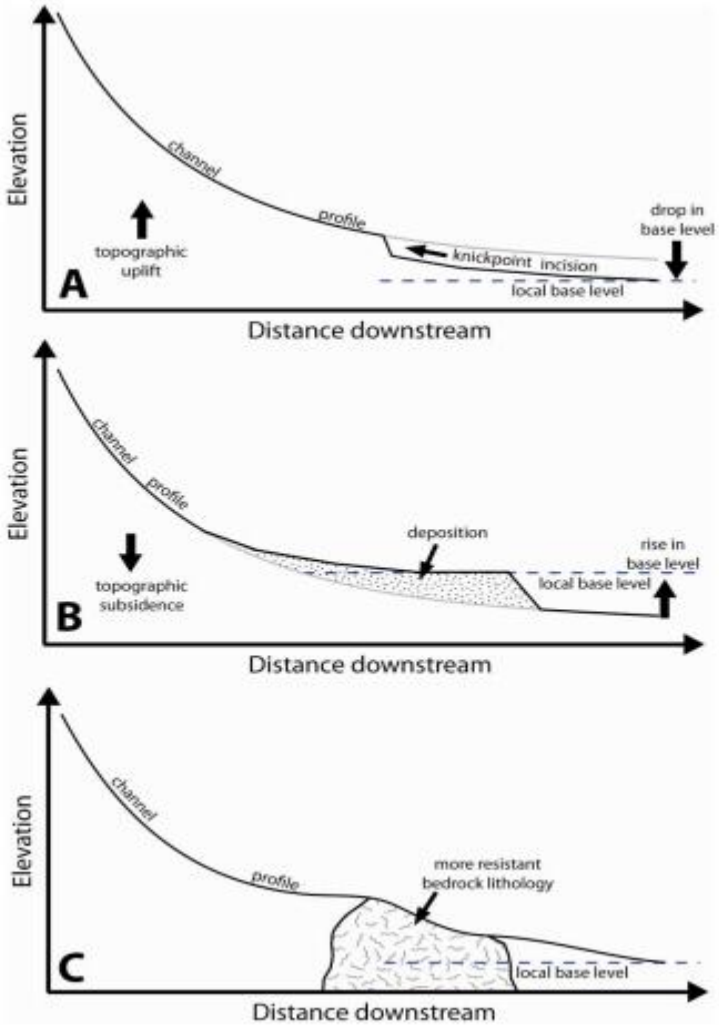

Figure 5: Perturbations to the longitudinal profile of a stream channel.

Source: Selander (2004)

From figure 5 above, (A) Relative drop in base level via tectonic uplift of the catchment or local base level fall.

(B) Relative rise in base level via tectonic subsidence of the catchment or local base level rise.

(C) Variations in downstream lithology.

Climate change affects the amount of water that is available to influence water in the channel network. It also directly affects the weathering processes that

take place in the channel, amount of sediments that move into the channel and the stream's capacity to move the sediment. The disparity in the competence of bedrock lithology underlying a channel will limit or enhance the channel's ability to incise vertically and produce local and reach scale changes, in channel slope measurements (Selander, 2004). Selander referred to these as the primary drivers and processes in the morphology of channel networks.

The morphology of a catchment is linked to the sediment flow within the catchment. Zwet (2012) iterated that the morphological behaviour of a catchment is determined by erosion and deposition of sediments within the catchment. Due to shear stress of wind and runoff, sediments are transported through the river as suspended sediments through the river system. Dust deposition from outside the catchment occurs by aeolian transport. Zwet (2012) considered the notion, in order to make a well-founded prediction of the siltation rate in the White Volta, it was relevant to comprehend the morphological behaviour of the catchment area. Van der Zwet took into consideration the flow of sediments in different branches, the origin of the sediments and how hamattan dust deposition is associated.

There have been several studies to show the channel morphology of rivers that show the stage of a river at a particular section at a particular point in time. This has influence on the knowledge of processes of rivers leading to various outcomes. Various investigators have noted that greater boundary resistance is associated with channels that have narrow, deep cross sections, a compound cross section with an inner channel, a steeper gradient with knickpoints or step-pool sequences, or a canyon with undulating walls (Wohl & Achyuthan, 2002). In

looking at the influence of substrates on incised-channel morphology, Wohl and Achyuthan established that there is a dramatic longitudinal transition in the channel geometry and erosional features between channel segments of differing substrate. Each section of the river channel experience varying processes leading to several differing features. Hence channel morphology gives information on the stages, processes and features that is likely to be present in that segment of the river environ.

Based on these findings, the White Volta river exhibits characteristics of rivers in the old age stage, revealing a lot of river features present among rivers in this stage. The features include meanders, scrolls, flood plains, oxbow lakes among others. These features are also influenced by anthropogenic factors. Other than a heavy down pour resulting in floods and avulsion processes, man-made factors such as the construction of dams, farming, irrigation and engineering works also cause changes in the channel morphology. Therefore, the channel morphology of rivers should also include anthropogenic influences and not only attributed natural causes.

Morphometric Analysis

Morphometric of the earth surface is the mathematical analysis of the earth's surface shape, dimension, configuration and landforms (Martins & Gadiga, 2015). Morphometric studies in the field of hydrology were first initiated by Horton (1940) and later Strahler (1957). The morphometric analysis of the drainage basin and channel network play an important role in understanding the geo-hydrological behaviour of drainage basin and expresses the prevailing climate, geology,

geomorphology, structural antecedents of the catchment. The relationship among various drainage parameters and the aforesaid factors are well recognized by many studies (Horton, 1945; Strahler, 1957; Nageswara, Swarn, Hari & Arun, 2010; El Bayomi, 2010; Pisal et al. 2013).

Analysis of the drainage basin is relevant to hydrological investigations as assessment of groundwater potential, groundwater management, pedology and environmental assessment. Hydrologists and geomorphologists have recognized that certain relations are almost important between runoff characteristics, and geographic and geomorphic characteristics of drainage basin systems. Several important hydrologic phenomena may be correlated with the physiographic characteristics of drainage basins such as size, shape, slope of drainage area, drainage density, size and length of the contributories.

In their study, Martins and Gadiga explained that Geomorphology had advanced over many years with quantitative physiographic means of depicting the characteristics of drainage network (including ephemeral networks). Erstwhile, the morphometric parameters were measured using mathematical concepts, but advanced technology used GIS modules which has provided a flexible environment and powerful tools for integrating, manipulating and analysing spatial information (Martins & Gadiga, 2015). Hence, without morphometric analysis, Martins and Gadiga postulated that, there was the risk of escalating the challenges of environmental management, underground water analysis, engineering projects, water pollution, and the health of the populace that benefited from the watershed.

Waikar and Nilawar (2014) have conducted morphometric analysis of the drainage basin in the Parbhani district of Maharashtra using Geographical Information Systems. Ramu and Jayashree (2013) used SRTM data to conduct morphometric analysis of the Tungabhadra drainage basin. Horton (1945) in his study of erosional development of streams and their drainage basins; hydrological approach to quantitative morphology, used morphometric analysis to describe streams and rivers in a quantitative term rather than describing them qualitatively. For example, a watershed can be well drained or poorly drained. While this description is vague, a better tool to Horton was to use the drainage density to describe the watershed. This approach has been widely accepted hence, being used by modern physical geographers. Therefore, there was the need to review these tools to better understand the river under study.

Mean Stream Length (Lsm)

The mean stream length is a characteristic property related to the drainage network and its associated surfaces (Strahler, 1957). The mean stream length (Lsm) has been calculated by dividing the total stream length of order by the number of stream.

Relief Ratio (Rh)

The relief ratio, (Rh) is ratio of maximum relief to horizontal distance along the longest dimension of the basin parallel to the principal drainage line (Schumm, 1956 (in Waikar & Nilawar, 2014). The Rh normally increases with decreasing drainage area and size of watersheds of a given drainage basin (Gottschalk, 1964).

Relief ratio measures the overall steepness of a drainage basin and is an indicator of the intensity of erosion process operating on slope of the basin (Schumm, 1956).

Relative Relief (Rbh)

Melton, 1957 (in Waikar & Nilawar, 2014) is the originator of the name. In the present study area, it is obtained by visual analysis of the digital elevation model prepared from Aster data. The elevation varies from -71m to 537m which represent the land has gentle to moderate slope.

Ruggedness number (Rn)

It is the product of maximum basin relief (H) and drainage density (Dd), where both parameters are in the same unit. An extreme high value of ruggedness number occurs when both variables are large and slope is steep (Strahler, 1957).

Areal Aspects

It deals with the total area projected upon a horizontal plane contributing overland flow to the channel segment of the given order and includes all tributaries of lower order. It comprises of drainage density, drainage texture, stream frequency, form factor, circularity ratio, elongation ratio and length of overland flow.

Drainage density (Dd)

Horton (1945), introduced the drainage density (Dd) as an important indicator of the linear scale of land form elements in stream eroded topography. It is the ratio of total channel segment length cumulated for all order within a basin to the basin area, which is expressed in terms of Km/Km^2.The drainage density, indicates the closeness of spacing of channels, thus providing a quantitative measure of the average length of stream channel for the whole basin. Some

literature revealed drainage density measurement made over a wide range of geologic and climatic type that a low drainage density is more likely to occur in region of highly resistant or highly permeable subsoil material under dense vegetative cover and where relief is low. High drainage density is the resultant of weak or impermeable subsurface material, sparse vegetation and mountainous relief. Low drainage density leads to coarse drainage texture while high drainage density leads to fine drainage texture (Strahaler, 1957).

Stream Frequency (Fs)

Stream frequency (Fs), is expressed as the total number of stream segments of all orders per unit area. It exhibits positive correlation with drainage density in the watershed indicating an increase in stream population with respect to increase in drainage density. The Fs for the basin is 1.59. (Horton, 1945)

Texture Ratio (T)

Drainage texture ratio (T) is the total number of stream segments of all orders per perimeter of that area (Horton, 1945). It depends upon a number of natural factors such as climate, rainfall, vegetation, rock and soil type, infiltration capacity, relief and stage of development.

Form Factor (Ff)

Form factor (Ff) is defined as the ratio of the basin area to the square of the basin length. This factor indicates the flow intensity of a basin of a defined area (Horton, 1945). The form factor value should be always less than 0.7854 (the value corresponding to a perfectly circular basin). The smaller the value of the form factor, the more elongated will be the basin. Basins with high form factors

experience larger peak flows of shorter duration, whereas elongated watersheds with low form factors experience lower peak flows of longer duration.

Circulatory Ratio (Rc)

Circulatory Ratio is the ratio of the area of a basin to the area of circle having the same circumference as the catchment. It is influenced by the length and frequency of streams, geological structures, land use/ land cover, climate and slope of the basin. A high value of circularity ratio shows the late maturity stage of topography (Kotei, Agyare, Kyei-Baffour, & Atakora, 2015).

Elongation Ratio (Re)

Schumm (1956) defined elongation ratio as the ratio of diameter of a circle of the same area as the drainage basin and the maximum length of the basin. Values of Re generally vary from 0.6 to 1.0 over a wide variety of climatic and geologic types. Re values close to unity correspond typically to regions of low relief, whereas values in the range 0.6–0.8 are usually associated with high relief and steep ground slope (Strahler 1957). These values can be grouped into three categories namely (a) circular (>0.9), (b) oval (0.9-0.8), (c) less elongated (<0.7).

Length of overland flow (Lg)

The Length of Overland Flow (Lg) is the length of water over the ground surface before it gets concentrated into definite stream channel (Horton, 1945). Lg is one of the most important independent variables affecting hydrologic and physiographic development of drainage basins. The length of overland flow is approximately equal to the half of the reciprocal of drainage density. This factor is

related inversely to the average slope of the channel and is quite synonymous with the length of sheet flow to a large degree.

Constant channel maintenance (C)

Schumm (1956) used the inverse of drainage density as a property termed constant of stream maintenance (C). This constant, in units of square feet per foot, has the dimension of length and therefore increases in magnitude as the scale of the land-form unit increases. Specifically, the constant C provides information of the number of square feet of watershed surface required to sustain one linear foot of stream.

Spatial Extraction of River Planform Features

Remote sensing applications becoming a prolific field of interest, the various uses are becoming common. The so called complex and vaguely understandable aspects of remote sensing and related applications such as GIS are gradually becoming a familiarity concept to which all factions of people are becoming acquainted with. Remote sensing processes are said to be complete when information of the earth surface is acquired and used for its intended purpose. The various platforms (ground, airborne and satellites) using mounted remote sensors record reflected energy as data for processing and analysis. With abundant information on the surface of the earth, a long list of applications is provided from remotely sensed data for various fields of application, including urban planning, disaster assessment and management, environmental monitoring and protection among others (Jia, 2015).

Information is a vital input for most developmental projects, planning, resource exploitation and others on regional and global scale. Land cover serves as a major source of such information and remote sensing is by far the cost effective and efficient method used to gather such huge data at a go (Minjie, et al., 2008). Therefore, our ability to process and analyse imagery from remote sensors allows us to monitor occurrences on the earth surface in real or near real time. However, extracting information from remotely sensed imagery is more difficult depending on the complexity of the landscape and the spatial and spectral resolution of the imagery. Improving the accuracy of the information extracted through image classifications is thus a fundamental topic of discussion (Minjie, et al., 2008).

Experts in trying to extract land cover information from data acquired from remote sensors consider spatial resolution to be more important than spectral resolution. Hence it is more useful to have finer spatial resolution (i.e. smaller pixel sizes) than higher spectral resolution (i.e. greater number of spectral bands or narrower interval of wave lengths). This has been a major justification for the use of aerial photographs in urban planning and management (Myint et al. 2010).

Sophisticated image classification processes are becoming highly popular within the remote sensing community. The classification process associates image objects with a proper class to which they belong and share similar properties and characteristics. This classification is a networked classes of image objects with specific relations to their objects in the class hierarchy. The classification of images can be subdivided into supervised and unsupervised, parametric and nonparametric,

hard and soft (fuzzy), or per-pixel, sub-pixel and per-field (Lu & Weng, 2007 cited in (Hayat, Bennamoun, & An, 2014).

The parametric classifiers postulate that the dataset is normally distributed and that its statistical parameters, which have been reproduced from the training of samples are representative (Ripley, 2007). Therefore, inadequate or multimodal distribution training samples can further introduce uncertainty to the image classification process. A second significant obstacle is the difficulty of integrating spectral data with ancillary data. On the other hand, non-parametric classifiers (Reineck & Singh, 2012)do not need the assumption of a normal distribution dataset (Hayat et al. 2014). As a result, non-parametric classifiers are uniquely befitting for the conjunction of non-spectral data into a classification procedure (Hayat et al.)

Usually, the classification technique used remains the prerogative of the user's specific demands, spatial resolution of the remotely sensed data adopted, and consistency with the work, image-processing and classification algorithms attainable, as well as the time frame. The training samples are usually collated from fieldworks, fine spatial resolution of aerial photos, and satellite images. Many factors such as spatial resolution of all images, assorted sources of data, a classification system, and obtainability of classification software should be considered while planning to adopt a procedure of classification. In this study, three classification methods are going to be examined.

Classification of Satellite Imagery

Digital image classification is the means through which information on the relationship between land cover and measured reflectance values from an image could be extracted. Two kinds of image classification approaches are available: supervised image classification and unsupervised image classification (Yan, 2003). Supervised classification is the process of using selected samples of known identity (training samples) to classify pixels of similar identity/digital number while unsupervised classification is the identification of natural groups, or structures within multi- spectral data by the algorithms available in the remote sensing software. For performing supervised classification, the software is trained on the features or pixels identified earlier to look for similar pixels throughout the image during the classification procedure (Dehvari & Heck, 2009). The training sets are clusters of homogenous pixels that designate a particular feature on the ground. Therefore, identification of similar pixels in the image automatically identifies similar existing ground surface features. Having a prior knowledge of the area of interest is very vital. Knowledge of the catchment characteristics is often acquired through field trips to the area (Thomas & Ayuk, 2010). For unsupervised classification on the other hand, there is no need to identify training sites of the area under study. The user is at liberty to choose the number of categories desired and the software classifies the image data into a number of groups of similar pixels corresponding to the number of categories stated earlier (Thomas & Ayuk). Both the supervised and the unsupervised methods of digital image classification have

advantages and disadvantages over each other. For this study, the supervised image classification technique was used as the major form of classification.

Pixel Based Classification

Pixel based analysis of remote sensing imagery can basically be in two main classifications, the supervised and unsupervised classification methods. In the past, most land use and land cover classifications were done using the pixel based classification (Weih & Riggan, 2010). Weih and Riggan explained that, with the pixel-based classification, the procedure analyses the spectral reflectance of the image by analysing every pixel within the area of interest regardless of the spatial or contextual information related to the pixel of interest. Hence each pixel that has been analysed can be put in a particular class of a theme based on its spectral reflectance. In recent times, images with higher resolution are becoming easier to assess and therefore making spatial information available to produce more accurate land use and land cover classifications.

Traditional classifications of images were based on the individual pixels. And this was a good recipe for relatively coarse spatial resolution images **(**Wang, Sousa, & Gong, 2004). Moreover, the land cover types to be classified most often are consistent with images with coarser scales. Higher spatial resolution images have an increase in the number of detectable sub class elements resulting in the intra class spectral variance which may lead to the separation of spectrally mixed land cover types more difficult (Wang et al.). But recent studies reviewed are revealing the uproar for object oriented classification over the traditional pixel

based classification mainly because it (pixel-based classification) is regarded as not suitable for very high resolution (VHR) images mainly because of the high spatial variability of pixels (Wang et al. 2004; Minjie et al., 2008; Myint et al. 2010). But all the same, algorithms are being improved to better classify images in the pixel based classifications as softwares are being updated more frequently.

Li et al (2014) tested fifteen algorithms under the pixel based classification which gave astonishing but closely related results. The algorithms included the Iterative Self-Organizing Data Analysis Technique (ISODATA) which is a popular advanced clustering algorithm, the Clustering based on Eigenspace Transformation (CBEST) an efficient k-means algorithm, the Logistic Regression which used the Ridge estimator, the Random Forest which has parameters using number of features and the number of trees in analysis, and the Maximum Likelihood Classification which estimates the mean and covariance matrix from training samples. Li et al findings revealed that while the other classification methods needed more than 200 samples per class to produce satisfactory results, the maximum likelihood classification only required 60 pixels to reach its highest accuracy. Other studies have also concluded that the maximum likelihood classification performed under the pixel based classification is most efficient and effective for classification. From this result, it has informed the selection of this method under the pixel based classification.

Object Based/Oriented Classification

The object oriented or object-based image classification (as often referred to) extends beyond the normal individual analysis of data points within a landscape by bringing together pixel-regions with regard to their spectral and spatial similarities (Watts & Lawrence, 2008). The result is an image object which serve as integrated units that exhibits an intrinsic scale and are made of structurally connected parts or pixels (Watts & Lawrence). Copious significant merits have been espoused in object-oriented classification over other methods for among the methods of classification.

Syed et al (2005) explained that with an object-oriented classified image, the basic picture elements were no longer the pixels, but rather interconnected groups of pixels (pixels that form an object). Therefore, it was evident that classification at this level thrived over the high-resolution problem and the salt and pepper effect in the pixel-based classification (Dehvari & Heck, 2009). According to Benz et al. (2004), these higher-level objects have spectral, textural, contextual and shape characteristics that can aid in classification. When the image is segmented, each group of pixels are measured based on the regions they are found and the relations that may exist between adjacent regions can be examined. The scale factor is indirectly associated to the average size of the objects to be detected (it has no unit). It is an abstract expression which defines the peak permitted heterogeneity within an image object (Mathieu et al, 2007). There is a deep-rooted inclination to idealize landforms with no guarantee of consistency of landform and feature mapping between individual mappers (Saha et al, 2011).

Li et al (2014) also used the object-oriented classification and it produced the best accuracies in terms of the classification method they employed. Even though they tested various algorithms under the classification method including the maximum likelihood classification, the Stochastic Gradient Boosting algorithm gave the best classification results. The object based classification experiments use algorithms that produce better results when the segment sizes are smaller. But Li et al (2014) concluded that with the increasing number of new algorithms being developed, there is the need to assess their performance and sensitivities to various kinds of environments. In order to satisfy this need, a standard image set with required classification scheme should be developed and sufficiently representative training and testing samples. To this effect, the study agrees with Li et al. knowing that the object based is not the only method of classification, it is indispensable to assess it against other methods, both improved and newly developed to find the effective algorithm of the time.

The advent of the object based classification has brought about a better way of image classification using various techniques, adaptations and total change in the algorithms used by pixel based classification. Many authors and GIS experts have diversified its use for a vast spectrum of purposes increasing the unlimited possibilities of image classification to their expected end. Therefore, object based image classification should be seen as a basic building block on which more advanced algorithms and classification techniques can be built upon.

Decision Tree Classification

Mishra et al. (2011) described decision tree as an inductive learning process that produces a classification tree with the help of training data/samples. This process is mainly a divide and conquer strategy to reach a specific class (Hastie, Tibshirani, & Friedman, 2009). Therefore, a class or feature in an image could only be classified by excluding it from the larger image. The exclusion could be a range of digital numbers or a band from a stacked image. Hastie et al (2009) explained this saying, the process involved the dividing of the training sets into subsets, and these subsets are subsequently divided repeatedly till it cannot be divided any longer. At this stage, it is known as the leaf. Like the actual tree which can have leaves even at the stem, a subset can also reach the leaf after the first division. It's a supervised classification method and its non-parametric nature allows it to be independent of the properties for the normal distribution of data (does not need to fit into the normal distribution curve) which makes it suitable for inclusion of non-spectral data into classification procedure. This is to ensure that a clearly defined class can be achieved. Another definition describes decision tree as "a set of conditions applied to intervals of features values" (Korting et al, 2010). The figure below shows a simple model of the decision tree.

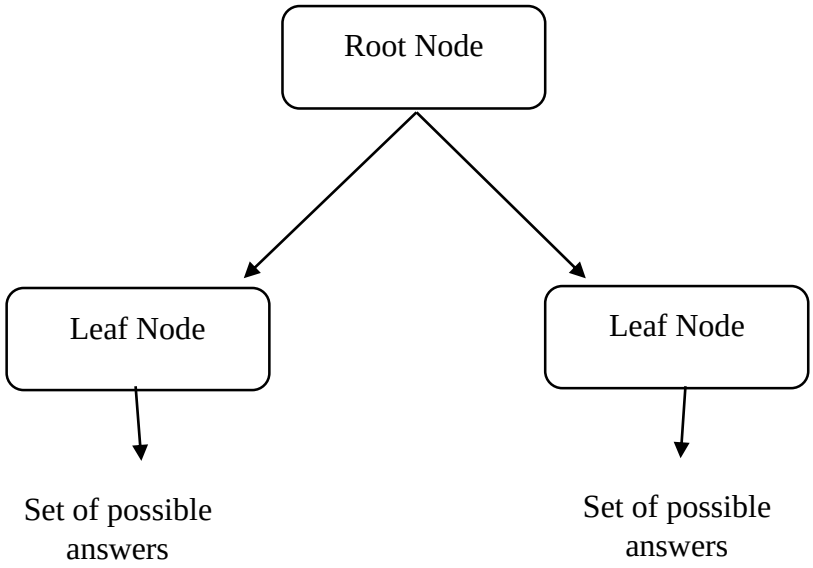

Figure 6: An example of a decision tree

Source: Korting et al (2010)

Each node corresponds to a non-categorical data and every connection means a data interval. The leaf in the tree means the categorical value expected if the path should follow through to that particular leaf from the root.

To construct a classification tree through a heuristic approach, there is the assumption that there is a data set consisting of feature vectors and their corresponding class labels are available. One is therefore able to identify the features based on problem specific knowledge. The construction of the decision tree is done by repetitive partitioning of the data into a homogenous/purer subset on the basis of a set of tests used for one or several attribute values at each branch or node in the tree. The procedure hence involves three steps including splitting nodes, determining which nodes are terminal and those that can be further split, assigning class label to terminal nodes. Assigning of class labels to terminal nodes is a straight forward activity; labels are assigned based on majority vote or weighted

vote when it is assumed that certain classes are more likely than others (Pal & Mather, 2001).

Pal & Mather (2003) demonstrated in their study the advantages of the decision tree for land cover classification in comparison with other classifiers such as the maximum likelihood method and artificial neural networks. Tooke et al, (2009) used decision tree to extract urban vegetation characteristics, including species and condition. Eric, et al. (2003) had examined the feasibility of using a decision tree as an instrument to map 11 land cover types. The DTC works to reduce both intra-class and inter-class variability through recursive binary splitting of training data values.

According to AIS & LUS (2000), Kheragarah tehsil of Agra suffers from many types of degradation such as salinity, waterlogging, ravines, degraded hills and rock quarries. In this study, an attempt has been made for identification, categorization and mapping of degraded lands of Kheragarah tehsil of Agra from remotely sensed data using decision tree classification. At the end of their study, Wei, et al., (2008) had this to say about the decision tree classifier in the Yellow River Delta area in Shandong China. An experimental study in the Yellow River Delta area showed that the proposed approach can reduce difficulty in classifying spectrally similar wetland classes, and consequently improve the classification accuracy. (Wei et al , 2008)

The decision tree classifier incorporated with remote sensing derived indices successfully distinguishes between different types of degradation. Moreover, it was found to be an efficient and useful approach for mapping land use

/ land cover. The study has demonstrated the superiority of the DTC over supervised classification (Mishra, Singh, & Yamaguchi, 2011). Hence, some advantages which DTC offers include its flexibility, simplicity, ability to handle noisy and missing data, lack of dependence on probability distribution function of data (Mishra et al.)

The methods for image classification become more comprehensive as new and better algorithms are being written down. The comparison of these methods therefore gives the researcher the upper hand to efficient classification and extraction of features in a given satellite image. A number of studies are able to compare images that have higher resolution and a classifier or two to bring out the method that best works on them.

Summary

The review sort to explain the concepts behind the meandering rivers, some features that resulted from them and the introduced a modern way of observing the phenomenon. It elaborated the reasons for the changing nature of rivers being associated with slope, velocity and volume. The earth observation and extraction methods are among numerous methods which have been used by many researchers to observe, plan and help formulate ideas for development or further studies.

CHAPTER THREE

MATERIALS AND METHODS

Introduction

This chapter presents the steps through which the study was conducted. It explains the philosophical basis of the methodology for this study as well as elaborates the methods used in the gathering data. The chapter explains the reason for the research design, the study area, the method data collection and the tools for analysis of data. It also highlighted the type of data collected and why it would be helpful in the analysis and the achievement of the objectives of the study.

Description of the study area

Location

The White Volta River Basin in Ghana is located between latitudes 8°50′N - 11°05′N and longitudes 0°06′E - 2°50′W. The basin is bounded to the east by the Oti River Basin, to the west by the Black Volta River Basin and to the south by the Lower Volta sub-basins. Burkina Faso forms its northern boundary. The drainage area of the White Volta River is about 50,000 km^2 (20% of Ghana's total land area), and constitutes about 44% of the total area of the White Volta River Basin (named Nakanbé River in Burkina Faso) (WRC, 2008). The White Volta River and its main tributaries in the northern part, the Red Volta (Nazinon) and the Kulpawn/Sissili

rivers, take their sources in the central and north-eastern portions of Burkina Faso (Andah, Van de Giesen & Biney, 2003).

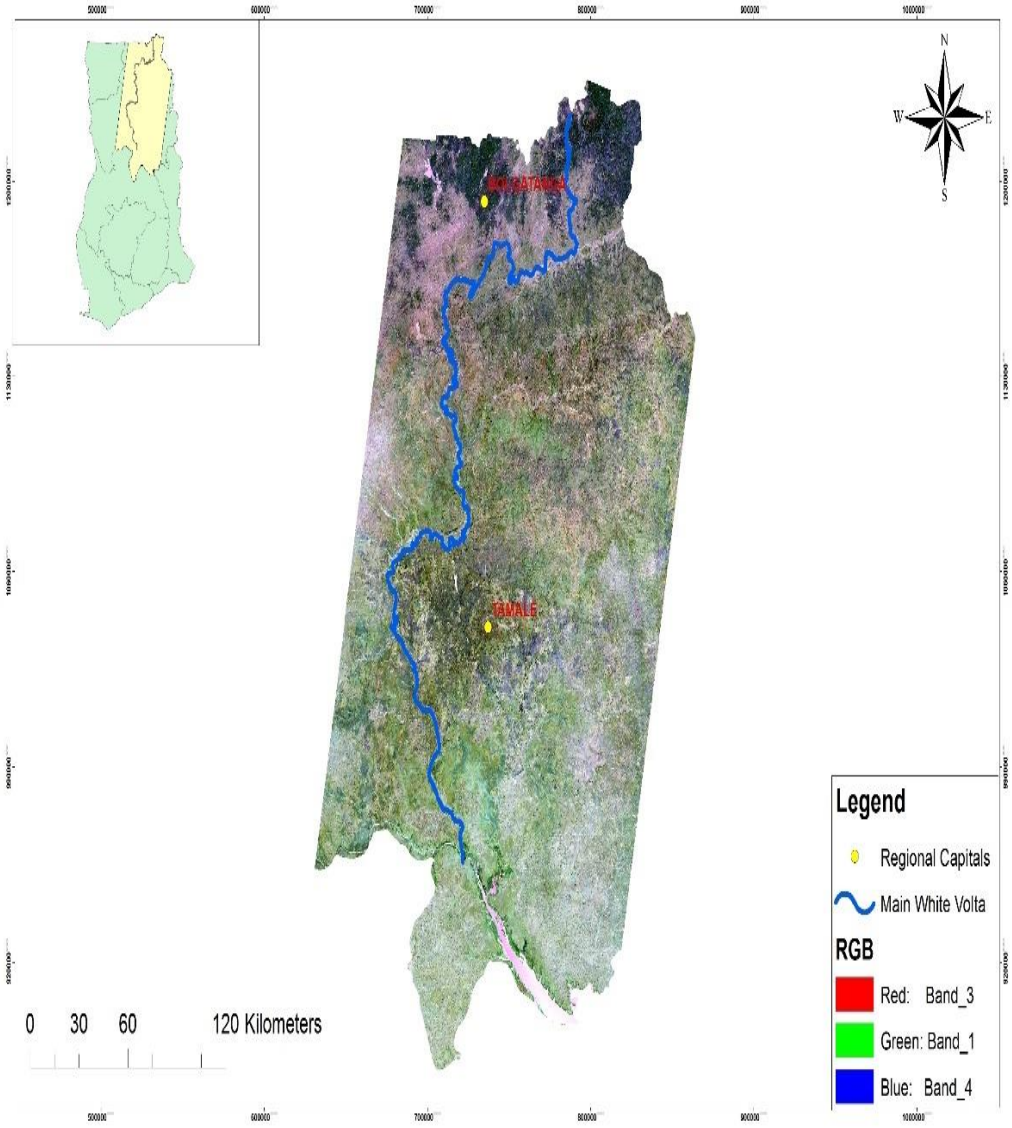

Figure 7: Map of the Study Area

Source: Author's Construct (2016)

Geomorphology and topography

The White Volta basin is characterised by fairly low relief with few areas of moderate elevation in the north and east. The average elevation is about 200 m and the highest portion reaches 600 m within the Gambaga hills in the northeast. The river initially flows southwards when entering Ghana, turns west to be joined by the Red Volta, continues westwards through the Upper East Region and then turns south, where it is joined by several tributaries, including the Kulpawn/Sissili and Nasia rivers. It continues southwards to Nawuni, flows westwards to Daboya and then southwards again where it is joined by the Mole river before entering the Volta Lake (Andah et al. 2003).

Climate and vegetation

The White Volta is located within a semi-arid tropic climate which is characterized by high temperatures and two distinct seasons, a dry season from October to April and the rainy season from May to September. The average annual temperature is 29ºC. The mean daily minimum temperature is 25ºC, coinciding with the peak of the rainy season, rising to a maximum of 34ºC in April (Abungba, 2013).

At present the vegetation of the basin includes shorter grasses and a few fire-resistant trees. This kind of vegetation has resulted mainly from prolonged grazing, burning and cultivation in the area. The north-eastern corner of the basin has been so disturbed by intensive farming that few other trees remain apart from the baobab (Adansonia digitata).

The traditional savannah woodland with light canopy which characterized the greater part of the area has gradually been replaced with a type of open savannah with scattered trees that rarely form closed canopy. Annual bushfires have acted to influence the dominance of grasses to the detriment of the former woodland. What remains of the original vegetation occurs along the wetter banks of rivers and streams as gallery forest and in fire protected forest reserves (WRC, 2008).

Land use

Predominant land use of the White Volta is extensive agriculture (land rotation cultivation) two to six miles away from the village with widespread grazing of large numbers of cattle and other livestock (up to 100 cattle/km^2). Farm sizes are usually less than 3 acres. Grazing lands are poor and are obtainable under natural conditions and annual bush burning (Abungba, 2013). Agriculture (including animal husbandry), fishery, hunting and forestry together constitute the main economic activity in the basin, particularly in the rural areas and provide occupation and employment for a vast majority of the people.

Agricultural activities are practiced both commercially and as subsistence farming. Improper farming practices such as slash and burn, and bush burning, are common practices (WRC, 2008). This results in further degradation of both the land and water resources of the basin. The cultivation of crops along river banks is also undertaken in many sections of the White Volta River, resulting in the removal of the top soil and increasing the risk of siltation in the river through upland erosion and subsequent transport of sediment into the open water courses.

Small scale industries and commercial activities include auto servicing shops, saw milling, carpentry, block making, local soap manufacturing and black-smith and metal working. In addition, manufactured goods are sold at large markets, which also form points of contact and trading connections between rural and urban residents.

Also, available to the communities are the presence of large and medium scale irrigation systems within the White Volta Basin and some can be found in the Tono (Kasina-Nankana District), Vea (Bongo District) and Bontanga (Tolon-Kumbungu District) localities. All the schemes are built on tributaries of the White Volta River and supply water primarily for the cultivation of rice and vegetables. There are also a number of small scale irrigation systems based on small dams, ponds and dug-outs in the basin. Another means of small scale irrigation farming – which is gaining popularity – is the use of portable water pumps to extract water from streams for watering of crops, i.e. mainly vegetables, in the dry season. This is practiced particularly along the main White Volta River, which in recent years has carried a rather steady dry season flow, as a result of the operation of the Bagré hydropower and irrigation dam in upstream Burkina Faso (WRC, 2008).

Harvesting of fuel wood and charcoal burning are important economic activities since the use of these for cooking is still predominant in both rural and urban homes within the basin. These activities result in further degradation of the basin's land resources (WRC, 2008).

Small-scale gold mining activities (galamsey) and stone quarrying are also common in some parts of the basin, particularly in the Upper East Region. In this

region, mining activities are undertaken mostly in the Nangodi area in the Talensi-Nabdam District, whereas the commercial stone quarrying activities are mainly centred around Pwalugu and Tongo also in the Talensi-Nabdam District (WRC, 2008).

Geology of the Basin

The Volta basin geology is dominated by the Voltaian system. But other geological formations present includes the Buem formation, Togo series, Dahomeyan formation, and Tertiary-to-Recent formations. The Voltaian system comprise of Precambrian to Paleozoic sandstones, shales and conglomerates. The Buem series is found between the Togo series in the east and the Voltaian system in the west consisting of calcareous, argillaceous, sandy and ferruginous shales, sandstones, arkose, greywacke and agglomerates, tuffs, and jaspers (UNEP, 2002). The White Volta Basin comprises the Birimian system and its associated granitic intrusives and isolated patches of Tarkwaian formation. According to Kesse (1985) (in Nyarko, 2007), all the formations within the White Volta basin with the exception of Dahomeyan series are under the super-group that happens to proceed from the Pan African orogeny which date from the late Proterozoic to Early Paleozoic. The Dahomeyan however on the other hand consists of the Cape Coast granotoids and Dixcove granotoids consisting of Potash, muscovite-biotite, granite and soda-rich hornblende biotite granite. Both divisions are of the Eburnean orogeny. It can be held from the above description that a greater percentage of the rocks of the White Volta are of sedimentary origin though some few are

metamorphic. Thus, sedimentation as a result of physical weathering is likely to be on the ascendency.

The long profile of the White Volta river showing a number of Knick points. The basin geology explains that the basin is dominated by sedimentary rocks. Hence the presence of several Knick points could be the aggradation of deposits of sediments. This provides evidence of flood peaks and low river levels. Zwet (2012) purported that, the velocity of rivers decreases as the river depth becomes shallow with vegetation. When the water level rises, its concentrated with sediments such that as the floodplains and river banks are filled, hence the receding water leaves a thick layer of sediments.

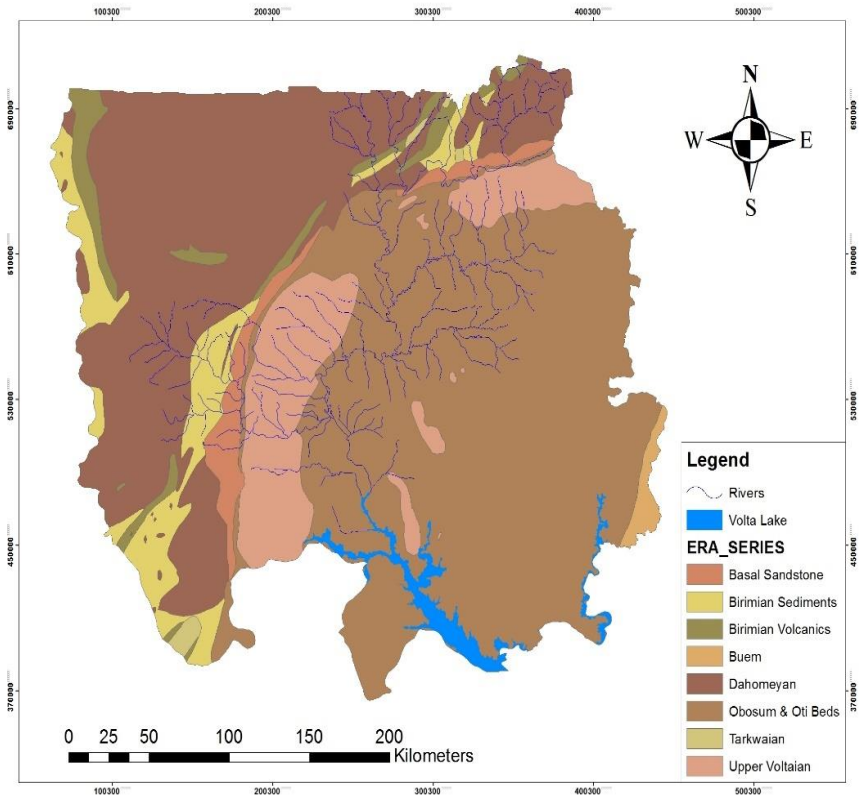

Figure 8: Superimposed drainage lines of the White Volta on the geology of the basin

Source: Author's construct (2016)

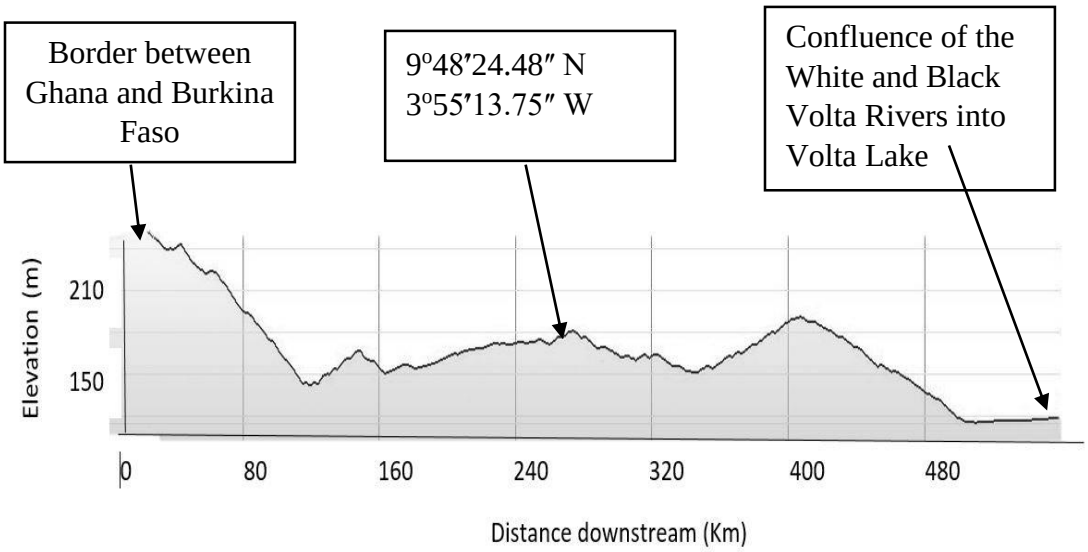

Figure 9: Long profile of the White Volta River

Source: Author's construct (2016)

Research Design

The study adopted the explorative study design focusing on the morphologic features present within the White Volta River basin. An explorative study seeks to gain a better understanding of the phenomenon, and serve as a basis to formulate theories (Creswell, 2012). The important phenomena in this case, the methods of extracting riverine features, are being studied or explored. It involved the use of quantitative techniques to analyse and interpret the types of riverine features that exist in the basin. Hence the use of the selected classification tools for analysis.

Sources and types of data

Satellite imagery of the riverine environment was downloaded from the United State Geological Survey (USGS) website (http://earthexplorer.usgs.gov/).

These images cover an extensive surface area at a time or wide surface aerial coverage. They also have a temporal resolution of sixteen (16) days, meaning the same surface could be captured after every sixteen (16). The principle behind these images is that land cover (river) characteristics are recorded as digital numbers or values in the image. The size of the area belonging to a pixel is called the spatial resolution. The image consists of spectral bands or layers (which is a characteristic of the sensor) that collect energy in specific wavelengths of the electromagnetic spectrum.

Three Landsat 8 Operational Land Imager (OLI) scenes were needed for the extraction of the river features in the study area because of the length of the river. Each satellite imagery consisted of 11 bands. The ancillary data, were obtained from the USGS website as well. The date for which the data was acquired was on the 14th of January 2016 (194; 054) and the 2nd of March, 2016 (194; 053 & 194; 052). This was within the dry season in which no significant change in land forms could have been recorded. Also, the images were the best scenes available for analysis regarding the free nature of data. The scenes were then reprojected to the Universal Traverse Mercator (UTM) Zone 30 North World Geodetic System of 1984 (WGS 84). This was done to correct the effect of the earth's curvature when projecting to a flat surface. The Advanced Spaceborne Thermal Emission and Reflection Digital Elevation Model (ASTER DEM) was also useful in the derivation of morphometric parameters and this was done using the hydrology toolbox in ArcGIS 10.3. The DEM data was reprojected into a projected coordinate

system. While the high-resolution images from google earth was used to help identify features being classified.

Table 1:Types of data used and their attributes

Data name	Pixel size in meter	File format	Type	Data source
Landsat 8 OLI	30	TIFF	Raster	http://earthexplorer.usgs.gov/
ASTER DEM	30	TIFF	Raster	http://earthexplorer.usgs.gov/

Source: Author's construct (2016)

The row and paths for the images are 194 & 052, 194 & 053 and 194 & 054 respectively for each set.

Image Pre-processing

The essence of image pre-processing is to eliminate the effect of the atmosphere in the remotely sensed image.

Atmospheric correction

The image was loaded with the metadata file into ENVI 5.1 and radiometrically calibrated. The FLAASH setting was used as the atmospheric correction module to convert the image values to radiance in order to get the surface reflectance of the image. The surface reflectance image was then scaled into a two-byte unsigned integers using a reflectance scale factor of 100,000. Therefore, the BandMath tool was used to divide the reflectance pixel values by 100,000 using the equation below. The output reflectance images were then used for further processing.

$$\frac{(B1\ le\ 0) * 0 + (B1\ ge\ 100000) * 1 + (B1\ gt\ 0\ and\ B1\ lt\ 100000) * float(B1)}{100000}$$

Where B1 represents each band of the image. (Nuhu, 2016)

Image processing

The image data at the time of acquisition, consist of eleven bandwidths capturing information at different wavelengths. The table below shows the wavelengths of Landsat 8.

Table 2:Landsat 8 bands and wavelength specifications

Landsat 8	**Wavelength (micrometers)**	**Resolution (meters)**
Band 1; Coastal aerosol	0.43-0.45	30
Band 2; Blue	0.45-0.51	30
Band 3; Green	0.53-0.59	30
Band 4; Red	0.64-0.67	30
Band 5; Near Infrared (NIR)	0.85-0.88	30
Band 6; Short-wave Infrared (SWIR) 1	1.57-1.65	60* (30)
Band 7; Short-wave Infrared (SWIR) 2	2.11- 2.29	30
Band 8; Panchromatic	0.50-0.68	15
Band 9; Cirrus	1.36-1.38	30
Band 10; TIRS 1	10.60 – 11.19	100* (30)
Band 11; TIRS 2	11.5- 12.51	100* (30)

*Band 6 is acquired at 60-meter resolution, but the images are resampled to 30-meter pixels.

Source: Landsat (2016)

The digital image processing done in the study involved image enhancement, image classification and post processing of classified images. However, the Landsat imagery (194 & 052, 194 & 053 and 194 & 054) went through the following processing techniques (rectification, projection changes, mosaicking, clipping and classification techniques) using ENVI and ArcGIS 10.3 for Image Analysis. The bands for the considered for the studies were bands 2, 3, 4, 5, 6and 7. For the sake of the environment to be worked in, a buffer zone of two kilometres (2km) was created to show the limit of the meandering river features. From the analysed data, it was identified that meandering river features were not presently seen in the image beyond 2km of the White Volta river, limiting the extraction of meandering river features to 2km on either side of the White Volta.

Digital Image Enhancement

Image enhancement techniques provide procedures that makes a raw image easier to interpret. In other words, these techniques improve the visual interpretability of the remotely sensed data to the human eye. Some image enhancement tools available in Envi 5.1 was used to improve the appearance of the image by adjusting contrast and brightness and using various contrast-stretch methods such as standard deviation, histogram equalization, maximum-minimum and density slicing (Thomas & Ayuk, 2010). The spatial enhancement (convolution, 3*3 and 7*7 kernel) was applied to the image to reveal the edges of features present in the environment.

Pixel-Based Classification

Green, Clark, Mumby, Edwards, & Ellis (1998) and Gao (1999) in their research had shown that among the various methods under the PBC, the maximum likelihood classification is the most effective method in classification. Wang et al. in 2004 adopted the method as a classification method at the pixel level as a starting point for their analysis. The MLC was the method selected under the PBC. First sample sites of the various land cover classes were selected (four for each class, summing to twenty samples). There were more than three sample regions selected and the average was calculated to derive the average reflection for each class. They were used to train the software to identify and categorise like spectral signatures under one class. The MLC then found the probability that each pixel fell into a particular class. The result was then clumped to create a better view of the classified image for comparison.

The MLC as a popular remote sensing classifier, corresponds a pixel to a class by means of its maximum likelihood. Hence, the likelihood (Lk) is defined as the posterior probability of a pixel belonging to class k.

$$Lk = P(k/X) = P(k) * \frac{P(\frac{X}{k})}{\sum P(i)*P\left(\frac{X}{i}\right)} \quad \text{..... Equation 1}$$

where P(k) = prior probability of class k

P(X/k) = conditional probability to observe X from class k, or probability density function. Usually P(k) are assumed to be equal to each other and P(i)*P(X/i) is also common to all classes. Therefore Lk depends on P(X/k) or the probability density function.

Therefore, a multivariate normal distribution function is applied as the probability density function. Given the case of the normal distribution, the likelihood can be expressed as follows

$$Lk(X) = \frac{1}{(2\pi)^{\frac{n}{2}}\{\sum k^{\frac{1}{2}}\}} exp\ \{-\frac{1}{2}(X-\mu_k)\ \sum_k^{-1}(X-\mu k)^t$$ ..... Equation 2

where n = number of bands

X = image data of n bands

Lk(X) = likelihood of X belonging to class k

μk = mean vector of class k

$\sum k$ = variance-covariance matrix of class k

$|\Sigma_k|$ = determinant of $|\Sigma_k|$

Object Based Image Analysis

Object oriented approach has been exceptionally efficient in the mapping of land cover and may be particularly useful in classifying wetland land cover and watersheds, as some studies have used in mapping wetlands. (Antunes, Lingnau, & Da Silva, 2003).

Obtaining information in the object based classification requires a basic step segmentation. The segmentation process splits an image into unclassified “object primitives” that form the basis for the image objects and the rest of the image analysis. A suitable scale factor was selected for the segmentation. The segmentation was then grouped into objects and inspected. This was used in the extraction of the features. The image processing software package used was Definiens eCognition, which is devoted to object-based image analysis. The

advanced attribution capabilities of eCognition is highly utilized on very high-resolution images (with pixel size less than or equal to 1 m) which gain increasing significance. The pixels are usually much smaller than image objects, therefore the interpretation of individual pixels is often not possible. As illustrated in the image C of figure 10, smaller pixels help to adequately group pixels that form the image for an enhanced interpretation. The images A and B have a low resolution and leads to generalising the pixel colour/shade, hence an improper representation of objects in the image. Segmentation cannot be ignored. As a result, OBIA has become the adequate tool of solution in many current tasks.

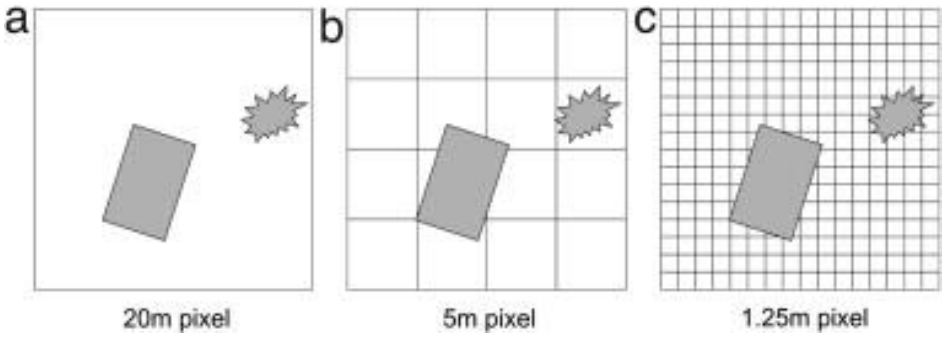

Figure 10; Relationship between objects under consideration and spatial resolution

Source: Blaschke (2010)

(a) low resolution: pixels significantly larger than objects, sub-pixel techniques needed. (b) medium resolution: pixel and objects sizes are of the same order; pixel-by-pixel techniques are appropriate. (c) high resolution: pixels are significantly smaller than object, regionalisation of pixels into groups of pixels and finally objects is needed (Blaschke, 2010).

Decision Tree

The rule-based classification of remotely sensed data using tree analysis for classification (also referred to as classification and regression tree analysis (CART), decision tree or the binary recursive partitioning) has been increasingly acknowledged. The tree analysis has exhibited the confidence for improving image classification accuracy in a number of studies done in recent times (Zambon et al. 2006; Elnaggar & Noller, 2010). The decision tree classification falls under the non parametric classification, which does not require the estimation of statistical parameters before classification (Mishra et al. 2011).

The decision tree is constructed with a training set consisting of objects which are described wholly by a set of attributes and a class label. The attributes refer to the collection of properties that store all information pertaining to the object in question (Ghose et al.2010).

To extract the physical information from backscattering behaviour of various object features, the analysis is based on polarized backscattering and cross-polar. These standard polarimetric features act as our information bearing features for predicting the nature of target. The study studied the images and came out with the range of pixel reflectance for the various features from the bands. The decision tree feature in Envi was activated by clicking “New decision tree”. The rule was then written to extract only water pixels and scroll bars. These were easily seen from the image.

Spectral angle mapper (SAM)

The spectral angle mapper classification is a classification algorithm that determines the spectral similarity between an image pixel and a reference spectrum in an n-dimensional feature space.

$$\alpha = cos^{-1}\left[\frac{\sum_{i=1}^{n} t_i r_i}{(\sum_{i=1}^{n} t_i^2)^{1/2}(\sum_{i=1}^{n} r_i^2)^{1/2}}\right]$$ ..... Equation 3

Where n = number of available spectral bands

t= pixel spectrum

r= reference spectrum

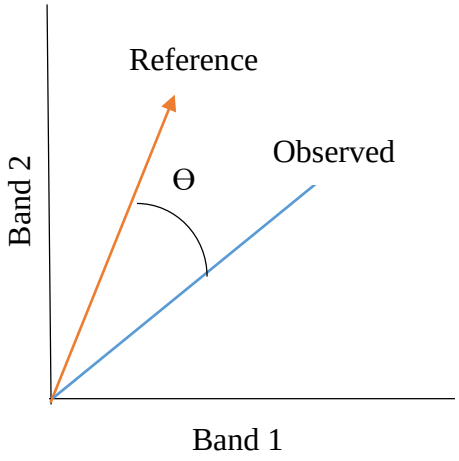

Figure 11: Representation of the SAM algorithm with two bands

Source: Nuhu (2016)

The reference spectrum is characterized by smaller angles and hence is represented by a pixel that exhibits the smallest spectral angle. Each band of each pixel can be considered as a vector which has a certain length and direction. The classification of the morphological features was done also using the SAM. SAM is a supervised classification technique that classifies an image using the known

spectral signatures of the classes i.e., endmembers. The endmembers could be taken from the laboratory, the field or extracted from an image (Nuhu, 2016).

Assessing Classification Accuracy

The accuracy assessment estimates the validity of the classification done in decimal which is then multiplied by 100 to convert it into percentage. The producer's accuracy is able to estimate the probability that a pixel in the ground truth library was correctly classified. While the user's accuracy focuses on estimating the probability of how well the classified object correctly predicts the correct class. The Over-all Accuracy (OA), is the number of correctly classified pixels (i.e., the sum of the diagonal cells in the error matrix) divided by the total number of sampled pixels.

$$Overall\ Accuracy = \frac{Number\ of\ correctly\ classified\ pixels}{Total\ number\ sample\ pixels} \ldots.$$ Equation 4

Every classified image in remote sensing would undergo an accuracy assessment. The assessment of a remotely sensed image is to compare and contrast its classified image. Every pixel in the image is compared with a reference source or a ground truth information (field confirmation). While this approach is ideal, gathering reference data for an entire study area is expensive (i.e., costly, labor intensive, and time consuming) and defeats the main objective of performing a remote-sensing classification (Lillesand, Kiefer, & Chipman, 2008). Therefore, a number of sample pixels that are assumed to represent the whole image are selected to avoid the above issue (Campbell, 2007; Jensen, 2005). Since accuracy assessment assumes that the sample points selected are the true representation of

the map being evaluated, an improperly gathered sample will produce meaningless information on the map accuracy (Congalton & Green, 1999; Jensen, 2005; Lillesand et al., 2008).

The preparation of an accurate map involved the use of remote sensing data and GIS techniques which, in turn, involved the use of multiple sources of digital data and other ancillary data sources supported by local knowledge of the area. The quality and accuracy of the output map was therefore being dependent on the quality and accuracy of the input data. A map accuracy check was performed using randomly selected sampling points in ArcMap as an event layer to ensure an even distribution for accuracy assessment. The Kappa value (coefficient of agreement) for the final map as a whole was also calculated. The Kappa coefficient is expressed in decimal and has a minimum of zero (0) and maximum of one (1) where the latter indicates complete agreement and is often multiplied by 100 to give a percentage (%) measure of classification accuracy (i.e. a kappa value of 0.89683 means that the total map accuracy is 89.68 %).

$$K = \frac{N \sum_{i=1}^{r} x_{ii} - \sum_{i=1}^{r} (x_{i+} \times x_{+i})}{N^2 - \sum_{i=1}^{r} (x_{i+} \times x_{+i})} \quad \text{.....Equation 5}$$

Where N is the total number of sites in the matrix, r is the number of rows in the matrix,

x_{ii} is the number in row i and column i,

x_{+i} is the total for row i, and

x_{i+} is the total for column i

The accuracy estimation was calculated using randomly sampled points generated in an Excel spreadsheet using the Analysis ToolPak extension. Minimum

and maximum values of x and y coordinates of the map were identified using ArcMap and using these values as a range, random data points for various locations were generated and displayed in ArcMap as an event layer (by adding the table as XY Landsat 8).

Root Mean Squared Error (RMSE)

The root mean squared error (RMSE) is a measure of the differences between known locations and locations that have been interpolated or delineated. The RMSE is a standard statistical metric to measure model performance in various studies (Chai & Draxler, 2014). The RMSE was used to compare the SAM model with the other three classifiers. The use of RMSE makes an excellent general-purpose error metric for numerical predictions.

$$RMSE = \sqrt{\frac{1}{n}\sum_{i-1}^{n}(y_i - \hat{y}_i)^2}$$ ……. Equation 6

Where n= the total number of reference points

y_i=the predicted location, $\hat{y}_i$=the actual location

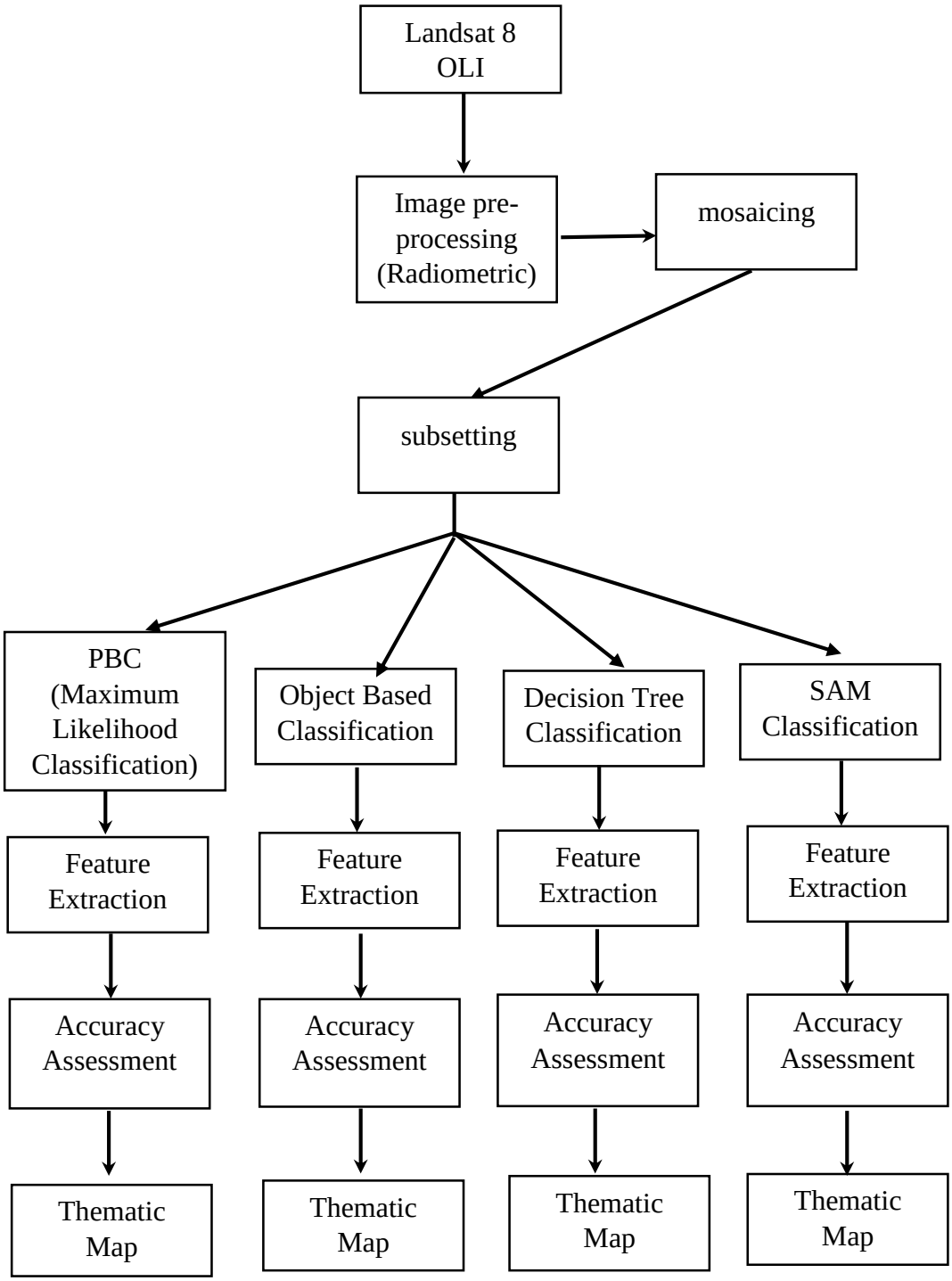

Figure 12: The flow chart of the work

Source: Author's construct (2016)

Morphometric Analysis

The three known determinants of running water systems operating in a basin are geology, relief and climate functioning at the basin scale. Using Geographic Information System (GIS) techniques for assessing various terrain and morphometric parameters of the drainage basins and watersheds provided a flexible environment and an important tool for the manipulation and analysis of spatial information (Hajam, Hamid, & Bhat, 2013). The Hydrology toolbox in ArcGIS was used for the calculation of the morphometric parameters. Table 4 shows the formulae and references for the various parameters that were calculated.

Table 3: Method of Calculating Morphometric Parameters of Drainage basin

Morphometric Parameters	**Formula/Definition**	**References**
LINEAR		
Stream order (U)	Hierarchical order	Strahler,1964
Stream Length (LU)	Length of the stream	Hortan, 1945
Mean stream length (Lsm)	$Lsm=Lu/Nu$; Where, Lu=Mean stream length of a given order	Hortan, 1945
RELIEF		
Basin relief (Bh)	Vertical distance between the lowest and highest points of basin.	Schumn,1956
Relief Ratio (Rh)	$Rh = Bh/Lb$ Where, Bh=Basin relief, Lb=Basin length	Schumn,1956

Ruggedness Number (Rn)	Rn=Bh×DdWhere,Bh= Basin relief, Dd=Drainage density	Schumn,1956
AERIAL		
Drainage density (Dd)	Dd=L/A Where, L=Total length of stream, A= Area of basin.	Hortan, 1945
Stream frequency (Fs)	Fs=N/A Where, L=Total number of stream, A=Area of basin	Hortan, 1945
Texture ratio (T)	T=$N1/P$ Where, N1=Total number of first order stream, P=Perimeter of basin.	Hortan, 1945
Form factor (Rf)	Rf=$A/(\mathrm{Lb})2$ Where, A=Area of basin, Lb=Basin length	Hortan, 1945
Circulatory ratio (Rc)	Rc=$4\pi A/\mathrm{P2}$ Where A= Area of basin, π=3.14, P= Perimeter of basin.	Miller,1953
Elongation ratio (Re)	Re=$\sqrt{(\mathrm{Au}/\pi)}/\mathrm{Lb}$ Where, A=Area of basin, π=3.14, Lb=Basin length	Schumn 1956
Length of overland flow (Lg)	Lg=$1/2\mathrm{Dd}$ Where, Drainage density	Hortan, 1945
Constant channel maintenance(C)	C =$1/\mathrm{Dd}$ Where, Dd= Drainage density	Hortan, 1945

Source: Walker & Nilawar (2014)

Meander geometry

While it is impossible to find rivers in a straight channel, rivers often develop meandering characteristics in alluvial plains. Therefore, the degree of meandering of a river is defined by the sinuosity (sinuosity greater than 1.5). Sinuosity that is always greater than unity increases with valley slope, but it reverts close to unity when braiding forms (Dey, 2014). Thus, meander geometry of rivers develops naturally to provide for the dissipation of the energy of moving water and the transportation of sediment.

Rivers continue to change in channel length (sinuosity) that result in maintaining a slope such that the stream system neither degrades nor aggrades. When the alignment of the river is adjusted, the geometry of the river also changes by reducing or increasing the natural sinuosity. The reach length changes causing local slope changes, and setting in motion a series of channel adjustments (Rosgen, 1996). The following geometric values were also measured.

Belt width: The meander belt width is the perpendicular distance between two meanders. Belt width is used as an index of the lateral containment or confinement of a stream when compared with the width of the channel. Meander Width Ratio (MWR) is the belt width divided by the bankfull width.

Meander length: the length of a meander is measured by the distance between two successive apex of meander.

Linear wavelength: The linear wavelength is the straight line joining two successive apex of meanders.

Radius of curvature: Radius of curvature is a measure of the "tightness" of an individual meander bend and is negatively correlated with sinuosity. Radius of curvature is measured from the outside of the bankfull channel to the intersection point of two lines that perpendicularly bisect the tangent lines of each curve departure point.

Channel width: This refers to the distance between two opposite banks at bank full level. The average width was calculated after taking measurements from different points along the channel.

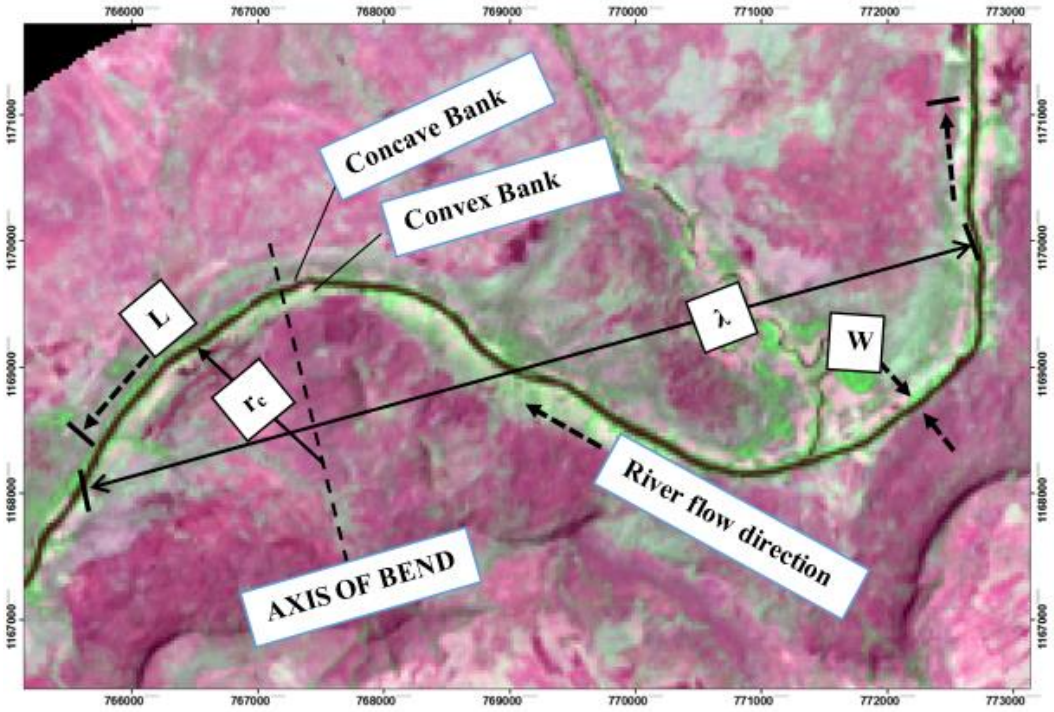

Figure 13: Meander geometry

Source: Landsat Image (2016)

L- Meander Length
r_c – Radius of curvature
W- Channel width
λ- Linear wavelength

Hence from figure 12, sinuosity can be calculated as: $S = \frac{L}{\lambda}$

Limitations of the Study

The study faced some challenges that were difficult to overcome while others needed a work around them. The major limitation of the study was that the study covered a vast area which was not accessible for field validation. The study therefore adopted the google earth imagery which have imagery captured in 2016 and were therefore valid as an alternate means for feature identification and validation.

Also, the processing time for each run was lengthy especially when using the Definiens' Ecognition software. The highest processing time for analysis was 28 hours continuous during which time the laptop could not be used for any other function.

CHAPTER FOUR

RESULTS AND DISCUSSION

EXTRACTION OF RIVERINE FEATURES FROM THE WHITE VOLTA RIVER

Results

The meandering features shown in the White Volta exhibit various shapes and sizes of riverine features with increased sinuosity and the results of separated lakes. The classification methods show the features resulting from the increased sinuosity as a result of riverbed instability as described by Dey (2014). Figure 14 shows the processed image before classification.

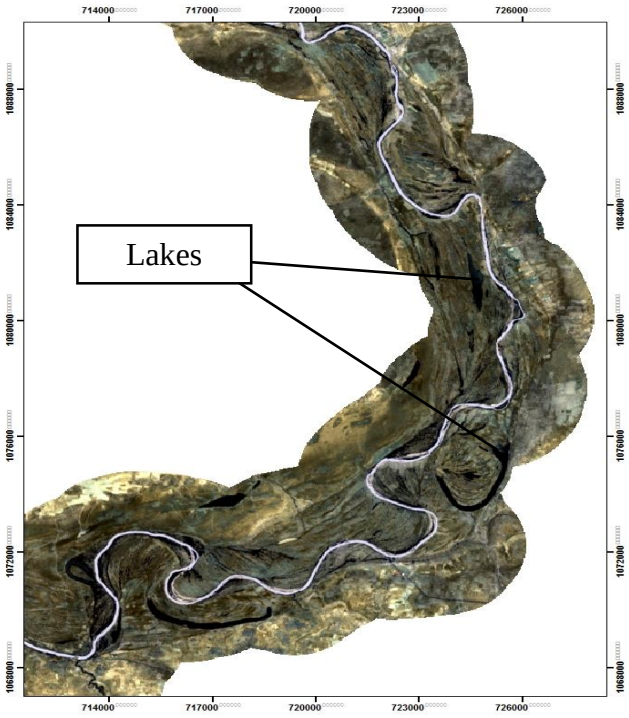

Figure 14: Figure showing a section of the White Volta with features
Source: Landsat Image (2016)

Landsat 8 OLI images of the White Volta river, was classified (using bands 5, 6 and 7) to extract the water cover map of the area using all the four classification methods mentioned where Maximum Likelihood, Decision Tree, Object Based Classifiers and the Spectral Angle Mapper. From literature, the maximum likelihood classification is most likely to record the lowest accuracy in classification schemes as selected in the study. This will therefore help to confirm or raise objections to what has been outlined in literature.

Maximum Likelihood Classification

The maximum likelihood classification was able to bring out the features such as the lakes, the river and some sediment deposits based on their spectral differences exhibited.

The lakes are the classification of interest to the study since a host of them are within the White Volta environment. The lakes covered a total of about 31.37 km^2 of the selected area. This classification includes all lakes natural that were located in the image as at the time it was captured within the dry season. These lakes are situated within the environs of the White Volta. They included oxbow lakes, lakes found in depression, and swamp lakes. The identification of these features was done with the high-resolution images from google earth. Hence the classification method was able to identify some features. The area of some of the features were also affected after the extraction. A possible reason could be attributed to the nature of this supervised classification method. This is because the

feature could be too small to be captured in the pixel or the feature had similar reflection to other features.

The river is less visible in the image unless zoomed into areas they can be located. The total area 63.6 km^2 equivalent to 70,665 pixels on the classified map. This refers to the main White Volta channel that was extracted. There were sections of the channel that were not extracted towards the north because of the narrow nature of the channel. This creates a gap given the impression of the break in flow of the river. This results from the fact that the Landsat 8 image resolution covers a wide area (30*30) and makes it difficult to capture clearly a river channel with a narrow width. Table 4 puts the area of coverage in perspective giving the area extracted in the image.

Table 4: Land cover classes and their area extent covered within the 2km buffer zone

Land Cover Classification	Number of pixels	Area in km^2
Main River	70,665	63.5985
Lakes	34862	31.3758
Features in Environment	17431	15.6879

Source: Classified Landsat image (2016), ENVI 5.1

The image after being classified exhibited the well-known salt and pepper effect identified by several researchers in their studies which prompted the need for a more efficient classification method which would have a higher accuracy. Wang et al. 2004 elaborated the shortfalls of the classification method, indicating that this method would not be preferred when the need to use a very high resolution image

arises. The reason is that the spectral variability in very higher resolution images are higher than in the Landsat 8 imagery. Hence, making the separation of spectrally mixed classes difficult. Apart from the disadvantage of low resolution Landsat image (Minjie et al., 2008; Myint et al, 2010; Wang et al) which was used in the study in the comparison of the classification methods, the extraction of the features using the supervised MLC most often are consistent with images with coarser scales.

Ancillary data was required to correctly identify the features extracted. Higher spatial resolution images have a higher number of detectable sub class elements resulting in the intra class spectral variance, which may lead to the separation of spectrally mixed land cover types more difficult (Wang et al. 2004). A more detailed section involving the White Volta and a two (2) kilometre buffer zone on each side of the river shows the features that were extracted from the image.

As indicated above, the coarse nature of the ML classification and the image resolution (30m, Landsat 8 OLI) does not make it suitable to properly view the various features amidst the noisy classification due to spectral inseparability. The study went a step further to reclassify the MLC in order to extract only water pixels and figure 15 shows the results.

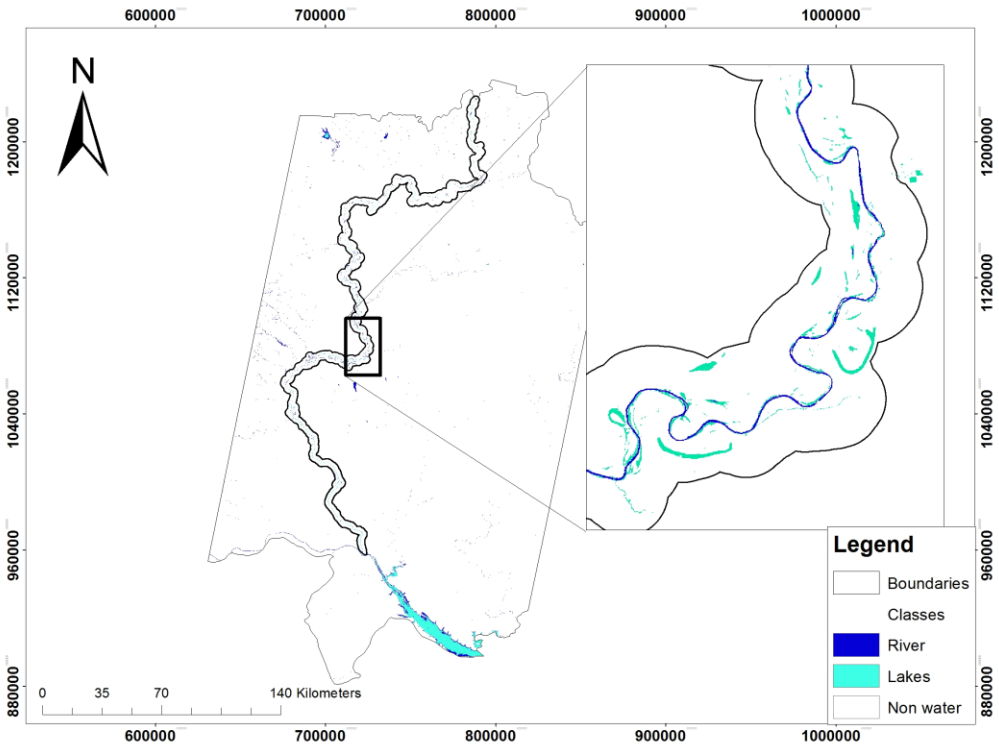

Figure 15: Map of reclassified MLC

Source: Classified Landsat Image (2016), Envi 5.1

Decision Tree Classification

Studies conducted with the decision tree classifier also included using sophisticated equipment coupled with very high-resolution (spatial) image data for their analysis. The area of the study is usually limited to a few squared kilometres. The decision tree as explained by Hastie, Tibshirani, & Friedman (2001) involved dividing training sets in the image consistently by different variables till the image cannot be divided further. This led to the extraction of water pixels in the image. And from this, the 2km buffer zone created from the image was used to clip out the region of interest where all the riverine features could be located. From table 5, it is evident that the area of the White Volta river including the features cover about

159.4 km^2 well within the estimated total area of the White Volta Basin by Water Resource Commission in 2008.

Table 5: The total water pixels within the region of the image and within the 2km buffer zone

Class	Total Pixels	Area in squared Kilometres
Main channel	78,957	71.061
Lakes	31,298	28.168
River features	66411	59.77

Source: Classified Landsat image (2016), ENVI 5.1

As shown in table 5, the extraction method allowed for the extraction of the water bodies in the image gives the researcher a fair idea of the total area covered by water bodies, that is 159km^2 within the catchment area. This shows a great increase in the area covered as compared to the supervised MLC. Examining the same features in the image, the DTC had some difficulty separating the main channel from the other lakes. This was explained through the subtle difference in the spectral variability of lakes and rivers because they all fall under the water class.

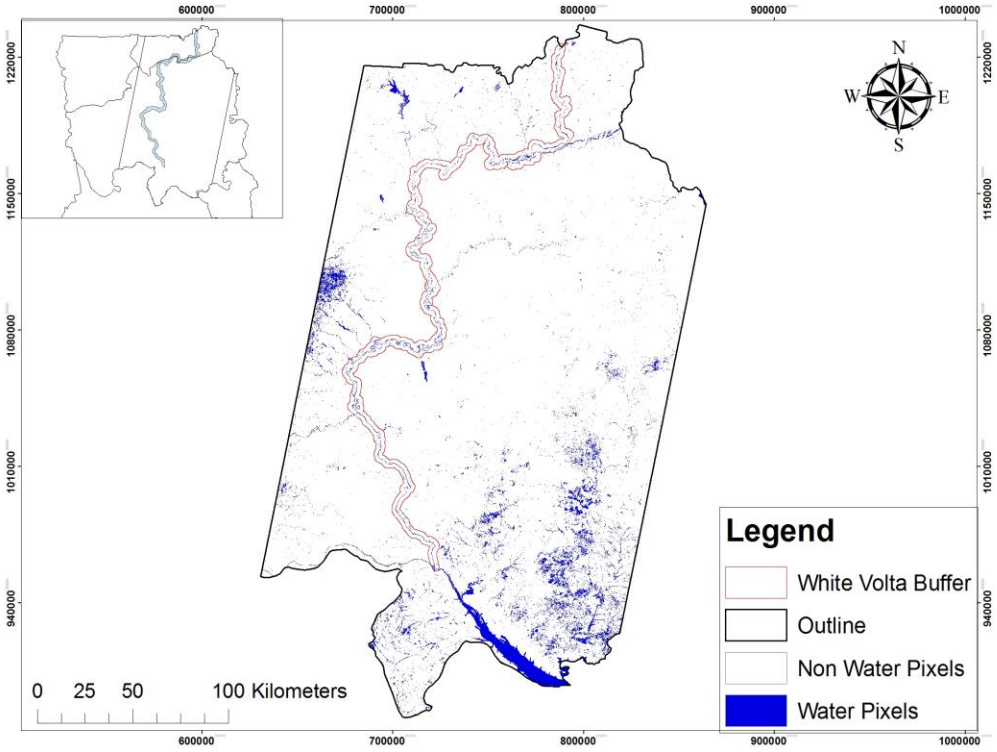

Figure 16: Map showing extracted features using the Decision Tree Classification.

Source: Classified Landsat Image (2016), Envi 5.1

From figure 16, the map shows only the water bodies that were extracted from the Landsat 8 image leaving all other features out. This is in line with what Mishra et al. (2011) listed as part of the advantages of the classifier, indicating that it omits the noisy nature as revealed in the MLC, it is flexible and simple. But it has been unable to extract the needed features for analysis.

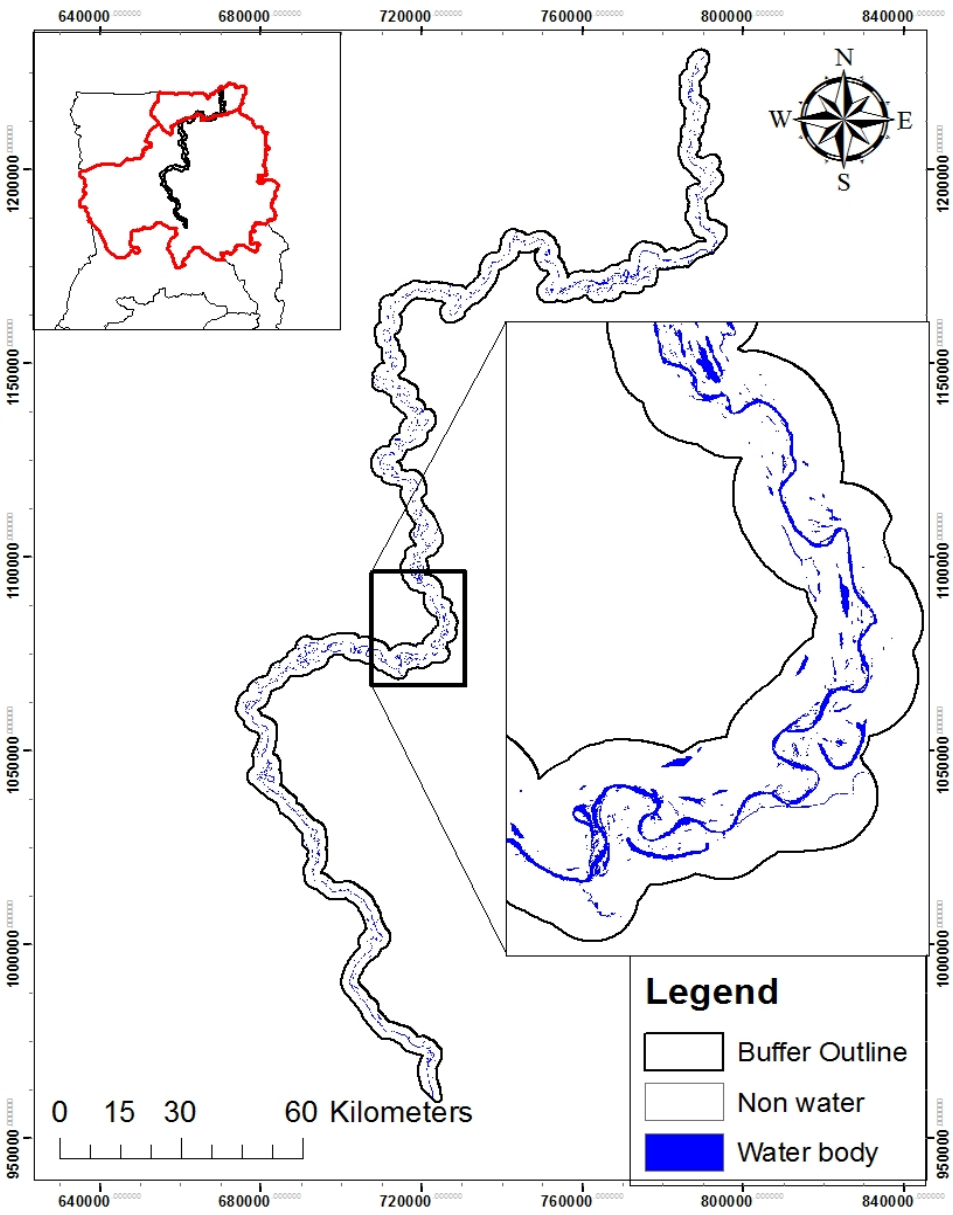

Figure 17: Map showing the extracted White Volta River and its environs using DTC within the 2km buffer zone.

Source: Classified Landsat Image (2016), Envi 5.1

Figure 17 shows the extracted riverine features in the White Volta environment. The river at this season is narrow characterized by the dry weather

conditions. As indicated the images were captured between January and March 2016.

Object-Based Classification

Watts and Lawrence (2008) in their studies revealed that the core of object based classifiers is its segments, hence they go beyond individual pixels to group them into meaningful objects there by bringing pixels with similar spectral and spatial similarities together. Figure 18 shows a map of the extracted river features in the Landsat 8 imagery with several pixel regions combined to form meaningful objects. With the improvement of classifiers after MLC, the noisy nature and the salt and pepper effect were taken out by the help of grouping pixels into regions giving the OBC an added advantage over the MLC and the DTC. The extracted imagery revealed much more features even with the nature of the Landsat imagery.

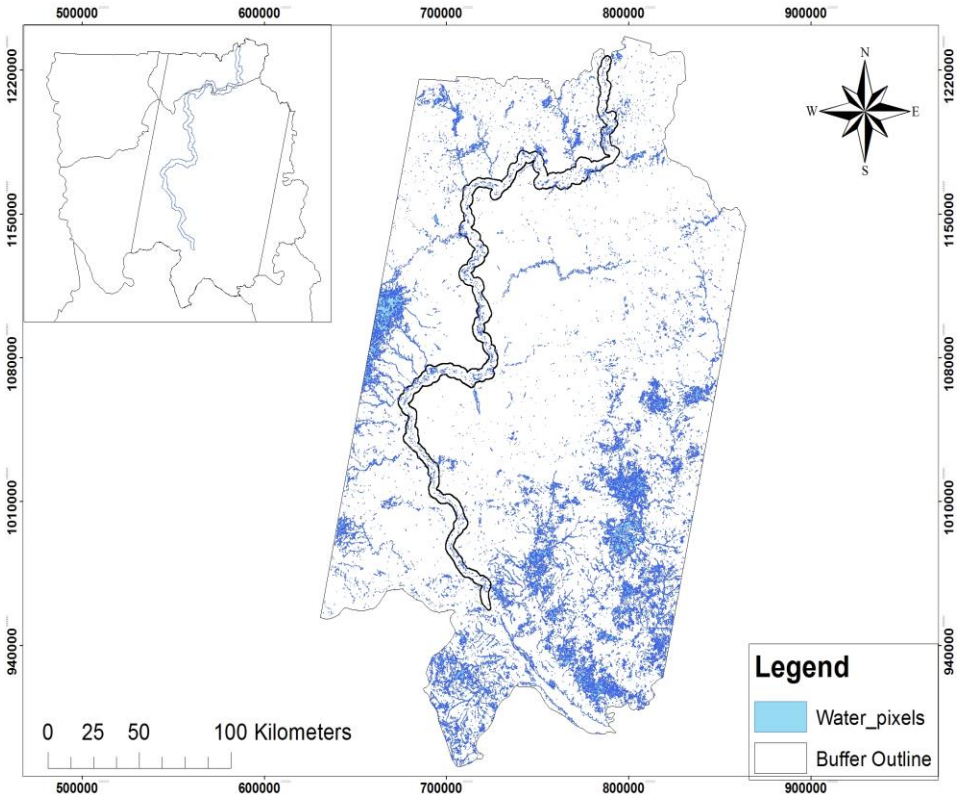

Figure 18: Map of the water bodies extracted using the object-based classification.

Source: Classified Landsat Image (2016), Envi 5.1

The study extracted the features that were present in the image including the escarpment shoulder in the north east of the image. As shown in figure 18, the extracted image gives a better view and correlation to river features as compared to the MLC. From figure 18, it is seen that several features representing various forms of lakes are present in the White Volta buffer zone revealing the numerous depressions storing water. The natural meandering features present were depleting mainly because of the rise in farming done close to the river as was the case when confirmed in the google earth imagery captured. Plate 1 gives a vivid illustration of this findings.

Figure 19:Picture showing modified meander feature as a result of farming

Source: Google Earth 2016

The Figure 19 below shows some extracted features of the Landsat 8 imagery using the object-based classification. It extracted much more features than the decision tree and the supervised MLC because of its ability to combine spectral, geometric and mathematical features to extract features in an imagery. The study found it to be superior to the other supervised MLC, DTC and SAM because of these abilities.

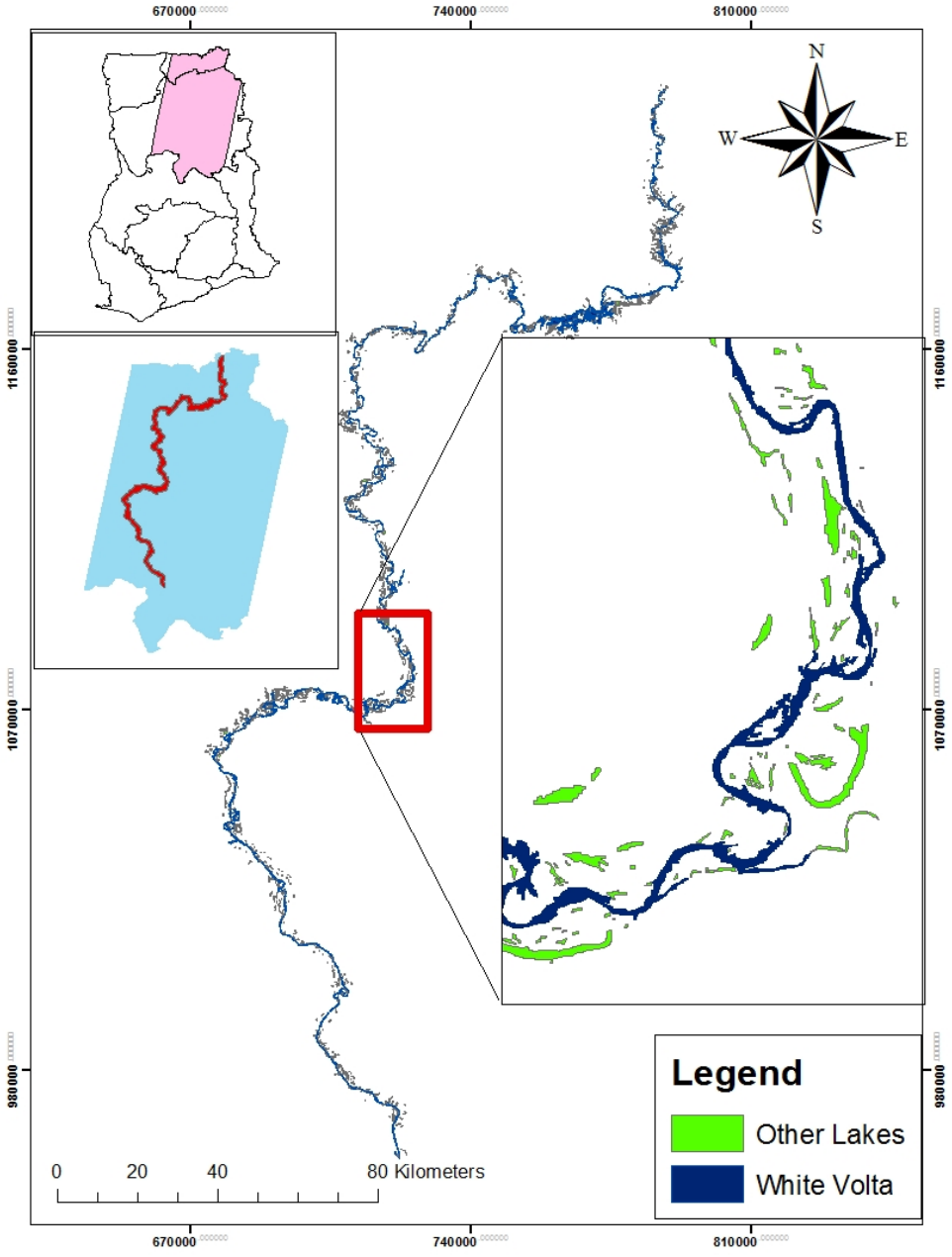

Figure 20: Map showing the extracted White Volta River and its environs using OBC within the 2km buffer zone.

Source: Classified Landsat Image (2016), Envi 5.1

Table 6:Table showing the total area of pixels displayed in the White Volta and its features using OBC.

Class	Total Pixels	Area in squared Kilometers
White Volta	110422	99.38
Lakes	44528	40.075
Other Features in Environment	61060	54.945

Source; Classified Landsat Image (2016), Ecognition Developer.

Table 6 gives the numerical break down of the area of the features in three which are the main channel (White Volta), the lakes formed around them and the features. The lakes are further divided into oxbow lakes and swamp lakes. With the ancillary data from google earth, the study identified meander scrolls as another major meandering feature present. This is consistent with Dey's (2014) study explaining a meander scroll as part of the meandering features. This is also evidence of river migration as well as the creation of oxbow lakes. Figure 21 below shows a part of the meandering White Volta with an oxbow lake to the right. It also shows meander scrolls within the oxbow and a careful look will show another swamp lake in the middle of the oxbow.

Figure 21: Picture showing an oxbow lake and meander scrolls

Source: Google Earth, 2016

Spectral Angle Mapper

The spectral angle mapper was able to extract the meandering features and show their extent to which they cover. Surprisingly, it had a better visual output than the MLC. The disadvantage of SAM is that, it classified the images of some scars as lakes rather than the scars. Figure 22 shows the image classification result after running the SAM algorithm.

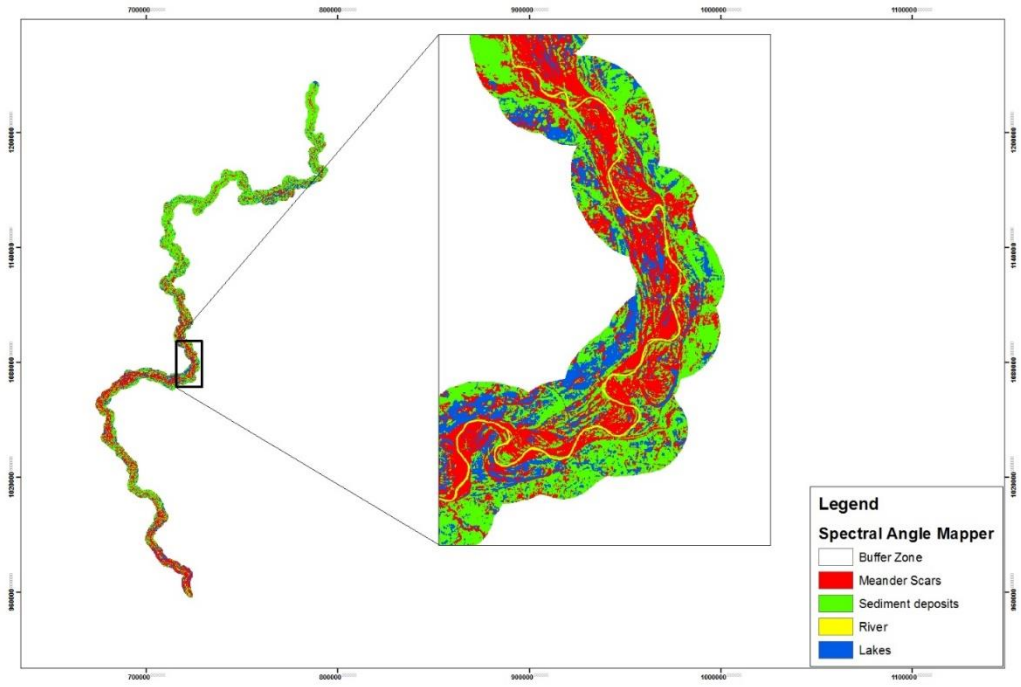

Figure 22: Figure showing the extracted features using the Spectral Angle Mapper
Source: Classified Landsat Image (2016)

Within the two-kilometre buffer zone, the sediment deposits showed the largest coverage to a size of close to 1350 km^2. This area also includes some sand bar features found within the concave bend of the river meanders. From figure 22, the image shows that the features represented were classified well to extract the meander scars. Table 7 gives the total areas covered by each class.

Table 7: Table showing the extent of area covered by the various classes using SAM

Classes	**Total Pixels**	**Km^2**
Meander scroll	823,886	741.5
Sediment deposits	1,499,822	1349.84
River	50,594	45.53
Lakes:	361,728	325.56

Source: Classified Landsat Image (2016)

From Table 7, the features show a larger total area size of lakes as compared to lakes extracted with the other methods. This on careful examination showed that the SAM classifier based on darker pixels as well classified some parts of the meander scrolls as lakes which inflated the area of coverage of the lakes.

Table 8: Table showing the total water pixels extracted within the White Volta Environs by each classifier

Classifier	**Total water Pixels within 2km buffer**	**Area in squared Kilometres**
Object Based	216,010	194.409
Decision tree	177,137	159.423
MLC	130,312	107.281
SAM	412,322	371.09

Source**:** Classified Landsat Image (2016)

From Table 8, the SAM is seen to have more extracted pixels of features and hence more area identified as part of the river and its features than the others. This is because the SAM is unable to differentiate between some features which have similar spectral angle. From the classification, the river and other parts that had similar class angles where classified as one. This raised the area classified to nearly twice the area of OBC, or more than twice in the case of PBC and DTC. This accounts for the higher error.

Accuracy Assessment

The accuracy of a classified/extracted image is calculated by dividing the number of class's pixels correctly classified over the total number of pixels belonging to that class. In other words, Accuracy= number of pixels assigned to the correct class /number of pixels that actually belong to that class. If this calculation is done for all of the classes together, the mean accuracy for all classes is calculated as overall accuracy. The accuracy assessment was calculated using generated random points that were exported to google earth imagery for assessment. Table 9 shows the confusion matrix of maximum likelihood classification.

Table 9:Table showing confusion matrix for MLC

Class	**Main River**	**Lakes**	**Meander scroll**	**Total**
Main River	365	39	7	411
Lakes	1	1471	100	1572
Meander scroll	0	21	9074	9095
Total	366	1531	9181	11078

Ground Truth (Pixels)

Source: Classified Landsat Image (2016)

The overall Accuracy for the MLC recorded was 98.48% with kappa Coefficient as 94.92% (0.9492). The user and producer accuracies are listed in Table 10.

Table 10: Table showing user and producer accuracy

Class	Producer Accuracy	User Accuracy
Main River	99.73	88.81
Lakes	96.08	93.58
Meander scroll	98.83	99.77

Source: Classified Landsat Image (2016)

Decision Tree Classification

The overall Accuracy of the DTC recorded was 99.89% with kappa Coefficient as 94.6% (0.9461). The table below shows the confusion matrix.

Table 11: Table showing the confusion matrix for DTC

Class	Rivers	Lakes	Other	Total
Class 1(Rivers)	56	6	18	80
Class 2(Lakes)	45	530	0	576
Class 3 (Meander scrolls)	0	0	65851	65851
Total	101	536	65869	66506

Source: Classified Landsat Image (2016)

Table 12: Table showing user and producer accuracy for DTC

Class	Producer Accuracy (%)	User Accuracy (%)
Class 1(Rivers)	55.45	70.00
Class 2(Lakes)	98.88	92.17
Class 4(Other)	99.97	100.00

Source: Classified Landsat Image (2016)

The decision tree classifier was able to produce outstanding accuracy results showing 98 percent and 94 percent for producer and user accuracy respectively. The overall accuracy stood at 99.89 percent and the kappa coefficient at 0.94 The high figures are as a result of the use of the SWIR 1 and 2 band combinations which has reflectance for water in the lowest range. Hence allowing the researcher to capitalize on this advantage to properly extract water bodies.

Object Based Image Analysis

The overall accuracy recorded by the OBC is 97.37%. While the kappa index of agreement was 95.05% (0.9505). The table below shows the confusion matrix of the OBC.

Table 13: Table showing object based image classification confusion matrix

	River	**Lake**	**Other Class**	**Sum**
River	4	0	0	4
Lake	0	9	0	9
Other Class	0	0	24	24
Unclassified	1	0	0	1
Sum	5	9	24	

Source: Classified Landsat Image (2016)

Table 14: Table showing user and producer accuracy for OBIA

	River	**Lake**	**Other Class**
Producer	0.8	1	1
User	1	1	1
KIA Per Class	0.8	1	1

Source: Classified Landsat Image (2016)

*KIA- Kappa index of agreement

The classification accuracy was evaluated using ancillary data such as the NDWI and google maps. Sample segments were imported into the working project by means of error matrix based on samples (Benz, et al., 2004) and linked to the corresponding classes to build the confusion matrix. The user, producer, overall and kappa index of agreement were generated for the classes.

Spectral Angle Mapper(SAM)

The total accuracy assessment for the SAM was 81.19% with a kappa coefficient of 64.36%. The table below shows the error matrix generated from the reference data.

Table 15:Table showing error matrix of SAM classifier

Classes	**Meander Scrolls**	**Sediment deposit**	**Rivers**	**Lakes**	**Sum**
Meander scrolls	41	8	3	6	58
Sediment deposit	7	26	4	0	37
River	0	1	4	0	5
Lakes	2	6	1	11	20
Sum	50	41	12	17	

Source: Classified Landsat Image (2016)

Table 15 is an error matrix showing the accuracy from the classes generated from reference points exported to google earth. The overall accuracy as well as the kappa coefficient was also generated from the error matrix.

Table 16: Table showing a comparison of accuracy among the classification methods

	MLC	DTC	OBIA	SAM
Overall Accuracy	98.48%	99.89%	97.37 %	81.19%
Kappa/KIA	94.92%	94.61%	95.1%	64.36%

Source: Author's construct (2016)

Table 16 shows the comparison of the overall accuracies and kappa coefficients of all four methods of classification. Comparing the overall accuracies show that the DTC was most accurate. But with the kappa coefficient, which preferred to the overall, the OBIA had the highest accuracy. This indicates that the kappa coefficient is more objective in measuring accuracy and hence preferred to the overall accuracy.

RMSE

The RMSE for the four methods were calculated and the results tabled below. The OBC recorded the lowest margin of error. The SAM has the highest error margin of 0.57 as compared to the others while the OBC had the lowest error margin of 0.5. Therefore, the higher error margin reflects the lower accuracy hence giving a solid evidence to support the accuracy assessment derived from the various classifications.

Table 17: Table showing the RMSE for each classification

	MLC	DTC	OBC	SAM
RMSE	0.553775	0.547723	0.503322	0.565073
Kappa/KIA	94.92%	94.61%	95.1%	64.36%

Source: Author's construct

A comparison of the RMSE and the kappa coefficient revealed a correlation with the accuracy assessment and error associated with such accuracies. Thus table 17 shows that as OBC and MLC recorded 95.1% and 94.9% of kappa coefficient respectively, they subsequently recorded a RMSE of 0.50 for OBC and 0.55 for MLC. Hence, a classification technique with higher kappa coefficient also had a lower RMSE and vice versa.

Morphometric Analysis

The morphometric analysis parameters calculated for each extraction method is explained below. The values obtained in the table followed the methods for deriving them as proposed by some researchers and were applied to this study area.

Mean Stream Length (Lsm)

The mean stream length is a characteristic property related to the drainage network and its associated surfaces (Strahler, 1957). The mean stream length (Lsm) has been calculated by dividing the total stream length of order by the number of stream.

Relief Ratio (Rh)

The relief ratio, (Rh) is ratio of maximum relief to horizontal distance along the longest dimension of the basin parallel to the principal drainage line (Schumm, 1956). The Rh normally increases with decreasing drainage area and size of watersheds of a given drainage basin (Gottschalk, 1964). The relief ratio for the MLC, DTC, SAM and OBC were 1.88, 1.88, 1.88 and 0.006 respectively. This shows that the area covered by the OBC were more extensive

than that covered by MLC, SAM & DTC. This could be explained by OBC's ability to cover even ephemeral streams as said by Martins and Gadiga (2015).

Relative Relief (Rbh)

This term was given by Melton (1957). In the present study area, it is obtained by visual analysis of the digital elevation model prepared from Aster data. The elevation varies from -71m to 537m which represent the land has gentle to moderate slope.

Ruggedness number (Rn)

It is the product of maximum basin relief (H) and drainage density (Dd), where both parameters are in the same unit. An extreme high value of ruggedness number occurs when both variables are large and slope is steep (Strahler, 1956).

Areal Aspects

It deals with the total area projected upon a horizontal plane contributing overland flow to the channel segment of the given order and includes all tributaries of lower order. It comprises of drainage density, drainage texture, stream frequency, form factor, circularity ratio, elongation ratio and length of overland flow.

Drainage density (Dd)

Horton (1945), introduced the drainage density (Dd) as an important indicator of the linear scale of land form elements in stream eroded topography. It is the ratio of total channel segment length cumulated for all order within a basin to the basin area, which is expressed in terms of Km/Km^2.The drainage density, indicates the closeness of spacing of channels, thus providing a quantitative measure of the average length of stream channel for the whole

basin. Hence, the drainage density calculated from the maps showed equal figure for OBC and DTC of 0.24 while MLC drainage density produced 0.25. Some literature revealed drainage density measurement made over a wide range of geologic and climatic type that a low drainage density is more likely to occur in region of highly resistant of highly permeable subsoil material under dense vegetative cover and where relief is low. High drainage density is the resultant of weak or impermeable subsurface material, sparse vegetation and mountainous relief. Low drainage density leads to coarse drainage texture while high drainage density leads to fine drainage texture (Strahaler, 1964).

Stream Frequency (Fs)

Stream frequency (Fs), is expressed as the total number of stream segments of all orders per unit area. It exhibits positive correlation with drainage density in the watershed indicating an increase in stream population with respect to increase in drainage density. The Fs for the basin is 1.59. (Horton, 1945)

Texture Ratio (T)

Drainage texture ratio (T) is the total number of stream segments of all orders per perimeter of that area (Horton, 1945). It depends upon a number of natural factors such as climate, rainfall, vegetation, rock and soil type, infiltration capacity, relief and stage of development.

Form Factor (Ff)

Form factor (Ff) is defined as the ratio of the basin area to the square of the basin length. This factor indicates the flow intensity of a basin of a defined area (Horton, 1945). The form factor value should be always less than 0.7854 (the value corresponding to a perfectly circular basin). The smaller the value of the form factor, the more elongated will be the basin. Basins with high form

factors experience larger peak flows of shorter duration, whereas elongated watersheds with low form factors experience lower peak flows of longer duration.

Circulatory Ratio (Rc)

Circulatory Ratio is the ratio of the area of a basin to the area of circle having the same circumference as the catchment. It is influenced by the length and frequency of streams, geological structures, land use/ land cover, climate and slope of the basin. A high value of circularity ratio shows the late maturity stage of topography (Kotei et al. 2015).

Elongation Ratio (Re)

Schumm (1956) defined elongation ratio as the ratio of diameter of a circle of the same area as the drainage basin and the maximum length of the basin. Values of Re generally vary from 0.6 to 1.0 over a wide variety of climatic and geologic types. Re values close to unity correspond typically to regions of low relief, whereas values in the range 0.6–0.8 are usually associated with high relief and steep ground slope (Strahler 1964). These values can be grouped into three categories namely (a) circular (>0.9), (b) oval (0.9-0.8), (c) less elongated (<0.7).

Length of overland flow (Lg)

The Length of Overland Flow (Lg) is the length of water over the ground surface before it gets concentrated into definite stream channel (Horton, 1945). Lg is one of the most important independent variables affecting hydrologic and physiographic development of drainage basins. The length of overland flow for MLC, DTC and OBC are 2.08, and 1.56 respectfully

Table 18: Table showing the morphometric parameters of the image, MLC, DTC and OBC

Sr. no	Parameter	Image Value	ML Value	DT Value	OB Value	SAM Value
1	Basin Area $(Km)^2$	2459	2459	2459	2459	2459
2	Perimeter (Km)	981	981	981	981	981
3	Drainage density(Dd) (Km/Km^2)	0.23	0.25	0.24	2	0.26
4	Stream frequency (Fs) (Km)	0.003	0.012	0.004	0.24	0.015
5	Relief Ratio (Rh)	1.88	1.88	1.88	0.006	1.88
6	Texture ratio(T) (Km)	0.007	0.011	0.08	1.88	0.011
7	Basin Length(Lb) (Km)	324	324	324	0.008	324
8	Basin Relief(Bh) (m)	609	609	609	324	609
9	Ruggedness number (Rn)	140.07	152.25	146.16	609	152.25
10	Form Factor (Rf)	7.59	7.59	7.59	146.16	7.59
11	Circulatory ratio (Rc)	0.032	0.032	0.032	7.59	0.032
12	Elongation Ratio (Re)	1.55	1.56	1.56	0.032	1.57
13	Length of overland flow (Lg) (Km)	2.17	2	2.08	1.56	2
14	Sinuosity (S)	2.054	2.22	2.19	2.08	2.24
15	Constant channel maintenance (C) (Km)	4.35	4	4.17	2.16	4.21

Constant channel maintenance (C)

The constant, in units of square feet per foot, has the dimension of length and therefore increases in magnitude as the scale of the land-form unit increases. Specifically, the constant C provides information of the number of square feet of watershed surface required to sustain one linear foot of stream. The constant channel maintenance recorded values for the MLC ($4ft^2$), DTC ($4.17ft^2$), OBC ($4.17ft^2$) and SAM (4.21) respectfully.

Sinuosity

River as described by Lohani (2008) and Dey (2014), are considered as sinuous when they fall within the range 1 and 1.5, where 1 indicates the straight nature of the river while 1.5 reflects the winding nature of the river. Beyond the 1.5 mark of sinuosity, the river is meandering. The study shows the results of the calculated sinuosity of the White Volta in the original image as well as in the thematic maps exhibited above.

A reason for high sinuosity is explained by Dey (2014) that meandering rivers migrate gradually resulting long meandering loops which increases the river length and consequently high recorded figures. The high sinuosity actually indicates that the meander has migrated far enough to eventually form a closed loop cutting the loop off to form an oxbow lake. Table 19 below shows the various morphometric parameters in comparison to each classification method.

Table 19: Meander Geometry

	MLC(km)	DTC(km)	OBC(km)
Belt width	2.88	2.06	2.09
Meander length	5.43	3.96	3.3
Linear wavelength	3.56	3.43	3.41
Radius of curvature	0.48	0.65	0.66
Channel width	0.14	0.18	0.21

Source: Author's construct (2016)

From Table 19, it is seen that the belt width recorded by the MLC far exceeds the DTC and the OBC. As the belt width indicates the part of the basin containing the meander, it appears from the table that the MLC might have a higher error as compared to the DTC and the OBC. The table also shows an inverse relationship between the geometry recorded by the MLC and those recorded by the DTC and OBC. This brings out the fact that even though the MLC and the DTC rely more on the pixel reflectance, the ability of the DTC to combine other classes of data to help in extraction makes it more aligned with the OBC which involves both the spectral reflectance and spatial resolution. Hence reflecting the statement of Hastie et al (2009) and Watts and Lawrence, (2008) who explained the DTC and the OBC respectively, relied not only on the spectral reflectance of pixels but on other bands or the spatial resolutions of the imagery.

Discussion

The results showed that classification of the Landsat 8 OLI data was successfully performed using the four selected classification methods with relatively high results for accuracy assessment. The image allows for the extraction of water bodies with a 30-m resolution and also calculate for NDWI. The NDWI was used because it is an index that is used for the extraction of open water features. It does this by suppressing all other features and enhancing the water bodies to allow for easy selection.

The confusion matrix revealed that the overall best classification among the three methods was the decision tree with overall accuracy of 99.89% followed by the object-based classification recording 97.4% and the maximum likelihood by 98.48%. In spite of the study recording high overall accuracies especially for decision tree and object-based classifiers, the study based on some additional factors from the morphological parameters and user perspective before arriving at the final decision of the most preferred method. Also, such high accuracies were accepted because the methods were concentrating on the extraction of river features which were dominated by water bodies and meander scrolls. Myint et al. (2011) explained in their findings after they performed accuracy assessment that the class that recorded the highest assessment was with the pool and lakes/ponds category. They recorded as high as 98% for producer accuracy and as high as 100% for user accuracy.

They explained that this was because there were not many pools and lakes/ponds in the study area, since the study area does not contain any recreational, residential and commercial areas. Consequently, from the outcome of this findings, it is possible that water features generally might have a high

accuracy in classification or extraction. But the study also acknowledges the inability of the decision tree classifier to extract lakes as well as the object oriented and the maximum likelihood classifiers were able to.

Secondly the DTC and MLC recorded a kappa coefficient of 94.6% and 72.2% respectively and the OBIA 95.04% for kappa index of agreement. This is often regarded as the true accuracy of the classification done. Hence in the use of accuracy assessment, the object based is ranked as the highest with the verdict of the kappa co-efficient.

Visual inspection of the classification results shows that the MLC is consistent in producing a salt and pepper effect in its image as compared to the DTC and the OBIA. This is consistent with the literature studied giving a confirmation on some reasons for the need for a better classification method.

The MLC is easier to use; in that it requires less complex procedure as compared to the DTC and the OBC. The decision tree is well able to extract water pixels best but has difficulty in distinguishing the types of water bodies especially if they have closely related reflectance or digital number values. It has the ability to exclude classified pixels from classification and hence eliminates the salt and pepper effect which is a major flaw in MLC. The decision tree classifier although was very efficient in classifying water bodies in the study area, was defective in distinguishing the major distinguishing feature, the lakes. The studies reviewed did not show any evidence of such capability by the DTC. Thus, it could be concluded that the DTC is challenged when distinguishing features of similar characteristics in a low-lying area like the White Volta Basin. It is also complex because it requires the user to know some command lines or ruleset in order to be able to execute a particular action.

The OBC also requires training like the DTC but is user friendly and not as complex as the DTC, but not as easy as the MLC. It has the advantage also of blending up to six bands in its “six-layer mix” function to better enhance viewing and possible proper feature identification even with the 30m resolution. It is able to group similar pixel regions for classification and to quickly reclassify when pixels are identified to be wrongly classified. It further allows for inclusion into a class with the classification is not able to capture the phenomenon. The OBC is able to distinguish between types of water bodies using the mean reflectance as the DTC, but it also uses the geometry, function which can use commands like the “relate border to image border” and “length” functions to distinguish between water bodies.

The SAM extracted more features showing evidence of the meander scrolls. But it has similar advantages and disadvantages like the MLC. It is easier to use when using the endmembers from the image rather than collecting endmembers from the field.

The major meandering features that were visibly extracted with ease were the oxbow lakes and other patches of water/lakes within a two (2) kilometre buffer zone created to examine them. It was established after the extraction water features in the image by all three classifiers that, meandering river features did not exceed that 2-kilometer distance measured in the image. The oxbow lakes ranged from the elongated crescent shaped ones to the ones that were almost coiled together such that the cut offs are almost closing to form rings of water. The other patches of water were best being explained as evidence of flood waters left behind in depressions.

The point bars and scroll bars were visible but could not be extracted on their own because they had similar reflectance to the ground surrounding them. This made every point and scroll bar feature extracted wrongly classified with the general ground surface.

CHAPTER FIVE

CONCLUSIONS AND RECOMMENDATIONS

Introduction

This concluding chapter gives the concluding remarks and possible suggestions that can be incorporated for various beneficial purposes. It concludes on the three classification methods used in the study explaining the outcome after experimenting with the methods to produce results.

Conclusion

The image used was a Landsat 8 OLI which has a thirty (30) metre resolution with eleven bands, except the panchromatic band which has a fifteen (15) metre resolution. The four major bands that were useful in the study were band 4 (Red), band 5 (NIR), band 6 (SWIR 1) and band 7 (SWIR 2). The combination of bands 4 and 5 were calculated to produce the NDWI for accuracy assessment while the combination of the three bands (Red, SWIR 1 and 2) were used in the RGB (false colour composite) in order to create a false colour composite image that clearly showed the edges of the water bodies. The resolution was too wide and hence distinguishing between built up surfaces and hard surfaces was nearly impossible.

In the first objective, the study sought to establish the fact that the methods would produce their own thematic maps with regards to extracting morphological features in the study area. The maximum Likelihood classification produced a thematic map of the area showing the various features

with the help of ancillary data. As found in the review of literature, the MLC after classification displayed a salt and pepper effect. The MLC achieved an overall accuracy of 98% which is very much consistent with what has been reported in literature regarding water classification in the majority. The possible explanation to this is that most literature used higher resolution images that were able to distinguish their features. Several studies were done using images from SPOT and IKONOS. In considering long features like the White Volta which stretches over several kilometres, the Spot and Ikonos might not be a cost effective choice. The decision tree displayed two (2) classes in its map output. The ability to separate water pixels from all other land cover types with ease was without the need to distinguish all other classes gives it an extra credit over the MLC. The DTC achieved an accuracy of 99.9%, which is almost a perfect score.

This is the result of extracting water bodies but as to distinguishing the water bodies is very difficult. The object based classification established three classes which were able to extract the water features that were required. The overall accuracy achieved for this was 97%. This was expected because of the high ability to segment image pixels into regions with similar reflectance values giving a high performance. And finally, the spectral angle mapper was able to extract all the features in the study area but had high errors in the output, as some classified areas were not part of the feature class it was associated with. SAM recorded the lowest accuracy and highest RMSE.

The accuracies recorded by each classification technique gave very high results. The study concludes that due to low image resolution, the various land cover classes were mixed and hence spectral variability was low. Hence it was

possible that a pixel could capture different features into one pixel. The pixel coverage was 900 m^2 (30*30) which was wide enough to capture several phenomena together.

Since both the decision tree and object based approach are non-parametric rules, they are independent of the assumption that data values need to be normally distributed. This is relevant because most data are devoid of normal distribution nature in many real-world situations. Another advantage of the object-based approach is that it allows additional and quicker selection or modification of new objects (training samples) each time after performing a classification until the satisfactory result is obtained. There are many possible combinations of different functions, parameters, features, and variables available with the object-based approach. The successful use of the object-based paradigm largely relies on repeatedly modifying training objects, performing the classification, observing the output, and/or testing different combinations of functions as a trial-and-error process. The SAM algorithm can be improved to reduce the error margin incorporated in the resultant classification images in order to improve classification. Finally, the classification methods have some level of subjectivity present because the user defines the parameters for all the methods.

The study's experience was that Definiens' eCognition software was not able to perform many features or bands at many different scale levels for image segmentation and classification. This was simply because the computer memory needs to be used extensively to segment tremendous numbers of objects from many different bands, especially when requiring smaller scale parameters (larger scale segmentation). The study used a fairly efficient computer hardware

(with 8GB RAM) and experienced numerous computer breakdowns and freezes during the segmentation.

This should be considered a limitation especially when dealing with a large dataset (finer resolution data for a relatively large area). Nonetheless, the object-based classification system is a better approach than the traditional per-pixel classifiers in mapping various distinguishing water features using high-resolution imagery given that it extracted the expected features and had the highest classification in what was expected.

Recommendations

The study after experimenting with the four methods made the following recommendations.

It recommends the use of the object based classifier in image extraction given the hardware conditions in use is fairly efficient.

Secondly, the extraction of features when considered should include digitizing the ground based features such as point and scroll bars in addition to the ancillary data.

The study also recommends that the use of a high spatial image resolution should be used on a section of the White Volta in order to observe the prevailing phenomenon acting on the water in situ.

The study further recommends the use of the decision tree in the classification of major or large-scale phenomena with the use of ancillary data. Even though the MLC had a low overall accuracy in comparison to the other two, it gave a remarkable high accuracy level indicating that it is not completely outdated. The study therefore recommends that the use of the MLC in image

classification or extraction is still credible only after the object based and the decision tree.

Finally, the use of SAM is relevant in morphological features and therefore can be improved to ensure a more accurate resultant feature

.

REFERENCES

Abungba, J. A. (2013). *Assessing the Impact of Agricultural Water Management on the Hydrology of the White Volta River Basin: The Case of Reservoirs and Dugouts.* Kumasi.

Abungba, J. A. (2013). *Assessing the Impacts of Agircultural Water Management Interventions on the Hydrology of the White Volta River Basin: The Case of Reservoirs and Dugouts.* Kumasi.

Agarwal, C. S. (1998). Study of drainage pattern through aerial data in Naugarh area of Varanasi district, U.P. *Jour. Indian Soc. Remote Sensing,26*, 169-175.

AIS & LUS, A. I. (2000). *Inventory or Degraded Lands of Agra district, U. P. using Remote Sensing techniques.* New Delhi: IARI.

Andah, W. E., Van de Giesen, N., & Biney, C. A. (2003). *Water, Climate, Food, and Environment in the Volta Basin* . Accra: Contribution to the project ADAPT Adaptation strategies to changing environments. ADAPT.

Antunes, A. B., Lingnau, C., & Da Silva, J. C. (2003). Object-oriented analysis and semantic network for high resolution image classification. *Anais XI SBSR, Belo Horizonte, Brasil, INPE*, 273–279.

Benz, U., Baatz, M., Dehghani, S., Heynen, M., Höltje, A., Hofmann, P., . . . Willhauck, G. (2004). *eCognition Professional 4.0 User Guide. Definiens Imaging.* Munich, Germany.: GmbH.

Blaschke, T. (2010). Object based image analysis for remote sensing. *ISPRS Journal of Photogrammetry and Remote Sensing* , 2–16 .

Campbell, J. (2007). *Introduction to remote sensing (4th ed.).* New York: The Guilford Press.

Chai, T., & Draxler, R. R. (2014). *Root mean square error (RMSE) or mean absolute error (MAE)? –Arguments against avoiding RMSE in the literature.* College Park: Geoscience Model Development.

Chapman, D. (1996). *Water Quality Assessments - A Guide to Use of Biota, Sediments and Water in Environmental Monitoring.*

Collison, J. (2016). *River and Watershed Restoration*. Retrieved from River and Watershed Restoration Website: https://riverrestoration.wikispaces.com/Channel+evolution+model

Congalton, R. G., & Green, K. (1999). *Assessing the Accuracy of Remotely Sensed Data: Principles and Practices.* Boca Raton: Lewis Publishers.

Couture, S. (2008, December 1). *River Dynamics and Erosion.* Retrieved from New Hampshire Government Website: http://des.nh.gov/organization/divisions/water/wmb/rivers/documents/designated_rivers.pdf

Cowan, A. M. (2013, March 21). *National Geographic Society*. Retrieved from Ocean Currents and Climate: http://nationalgeographic.org/media/ocean-currents-and-climate/

Creswell, J. W. (2012). *Educational Research: Planning, Conducting, and Evaluating Quantitative and Qualitative Research.* Lincoln: Pearson.

Davranche, A., Lefebvre, G., & Poulin, B. (2010). Wetland monitoring using classification trees and SPOT-5 seasonal time series. . *Remote Sensing of Environment* , 114, 552-562.

Dehvari, A., & Heck, R. J. (2009). Comparison of object-based and pixel based infrared airborne image classification methods using DEM thematic layer. *Journal of Geography and Regional Planning Vol. 2(4)*, 86-96.

Dey, S. (2014). *Fluvial Hydrodynamics.* Berlin Heidelberg: Springer-Verlag .

Dey, S. (2014). Fluvial Processes: Meandering and Braiding. *GeoPlanet: Earth and Planetary Sciences*, 529-562.

El Bayomi, G. (2010, June 17). Morphometric Analysis in Esna Basin Using Remote Sensing and GIS Techniques. *US-Egypt Workshop on Space Technology and Geo-information for Sustainable Development*. Cairo, Egypt.

Eric, C., Colstoun, B. d., Michael, H. S., Craig, T., Kathy, C., Timothy, G. S., & James, R. I. (2003). National Park vegetation mapping using multitemporal Landsat 7 data and a decision tree classifier. *Remote Sens. of Envi*, 85: 316-327.

GAO, J. (1999). A comparative study on spatial and spectral resolutions of satellite data in mapping mangrove forests. . *International Journal of Remote Sensing,*, 14, 2823–2833.

Google Earth, U. D. (2016). Google Earth Imagery. 2016.

Gottschalk, L. (1964). Generalization in the Writing of History. *Journal of Philosophy*, (18) 538-543.

Green, E. P., Clark, C. D., Mumby, P. J., Edwards, A. J., & Ellis, A. C. (1998). Remote sensing techniques for mangrove mapping. *International Journal of Remote Sensing*, 5, 935–956.

Hajam, R. A., Hamid, A., & Bhat, S. (2013). Application of Morphometric Analysis for Geo-Hydrological Studies Using Geo-Spatial Technology –A Case Study of Vishav Drainage Basin. *Hydrol Current Res* , 4: 157. doi:10.4172/2157-7587.1000157.

Hans-Henrik, S. (1996). River Meandering as a Self-Organization Process. *Science*, 1710-1713.

Harman, W. H., Tweedy, K. L., Hunt, W. S., Calmbacher, J., Norton, T., Van Stell, K., & Kaiser, C. H. (2013). *Natural Channel Design Protocol.* San Antonio.

Hastie, T., Tibshirani, R., & Friedman, J. (2001). *The Elements of Statistical Learning - Data Mining, Inference and Prediction.* New York: Springer.

Hawley, R. J., Bledsoe, B. P., Stein, E. D., & Haines, B. E. (2012). Channel Evolution Model of Semiarid Stream Response to Urban-Induced Hydromodification. *Journal of the American Water Resource Association*, 1-23.

Hayat, M., Bennamoun, M., & An, S. (2014). Object-oriented and Decision tree classifications for LULC using Cosmo-SkyMed, QuickBird and Landsat 7 satellite data: An Example of Erbil/Iraq. . *In Proceedings of the IEEE Conference on Computer Vision and Pattern Recognition*, (pp. pp. 1907-1914). Dresden, Germany.

He, X., Yan, S., Hu, Y., Niyogi, P., & Zhang, H. J. (2005). Face recognition using Laplacianfaces. *IEEE transactions on pattern analysis and machine intelligence*, 27(3), 328-340.

Hecher, J., Filippi, A., Guneralp, I., & Paulus, G. (2012). Extracting River Features from Remotely Sensed Data: An Evaluation of Thematic Correctness. *(Doctoral dissertation, Department of Geography, Texas A&M University).*, 187-196.

Horton, R. E. (1945). Drainage Basins; Hydrophysical Approach to Erosional Development of Streams and Their Quantitative Morphology. *Geological Society of America Bulletin 56.3*, 275-370.

Howard, A. D., & Knutson, T. R. (1984). Sufficient conditions for river meandering: A simulation approach. *Water Resources Research*, 1659-1667.

Immoor, L. (2006). *Classifying Rivers- The Three Stages of River Development.*

Jensen, J. R. (2005). *Introductory digital image processing: A remote sensing perspective (3rd ed).* Upper Saddle River: Prentice-Hall.

Jia, Y. (2015). *Object-Based Land Cover Classification with Orthophoto and LIDAR Data* . Stockholm.

Julien, P. Y. (1985). *Planform Geometry of Meandering Alluvial Channels.* Collorado.

Julien, P. Y. (1985). *Planform Geometry of Meandering Alluvial Channels.* Colorado.

Korting, T., Fonseca, L., & Camara, G. (2010). Decision Trees to Detect Changes in Remote Sensing Image Time Series. *National's Institute for Space - Image Processing Division*, 1-6.

Kotei, R., Agyare, W. A., Kyei-Baffour, N., & Atakora, E. T. (2015). Morphometric Analysis of the Sumanpa River Catchment Mampong-Ashanti in Ghana. *ARPN Journal of Earth Sciences*, 67-75.

Kurmis, P. (2002). Orthopaedic utilisation of three dimensional image displays reconstructed from magnetic resonance imaging. *Radiographer: The Official Journal of the Australian Institute of Radiography, Vol. 49, No. 2*, 67-71.

Landsat, A. (2016, January 15). *Frequently Asked Questions about the Landsat Missions*. Retrieved from US Geological Survey Web site: http://landsat.usgs.gov/band_designations_landsat_satellites.php

Langbein, W. B., & Leopold, L. B. (1970). River meanders and the theory of minimum variance. In Rivers and river terraces. *Palgrave Macmillan UK.*, 238-263.

Lazarus, E. D., & Constantine, J. A. (2013). Generic theory for channel sinuosity. *Proceedings of the National Academy of Sciences of the United States of America,*, 8447-8452.

Li, J., Carlson, B., & Lacis, A. (2014). *Application of Special Analysis Techniques to the Intercomparison of aerosol data -Part 4: Synthesized analysis of multisensor satellite and ground based AOD measurements using combined maximum covariance analysis.* . New York: Atmospheric Measurement Techniques.

Lillesand, T. M., Kiefer, R. W., & Chipman, J. W. (2008). *Remote sensing and image interpretation.* New York: John Wiley and Sons.

Lohani, M. (2008). *Effects of Stream Order and Data Resolution on Sinuosity using GIS.* Thesis: Unpublished.

Martins, A. K., & Gadiga, B. L. (2015). Hydrological and Morphometric Analysis of Upper Yedzaram Catchment of Mubi in Adamawa State, Nigeria. Using Geographic Information System (GIS). *World Environment*, 63-69.

Mathieu, R., Aryal, J., & Chong, A. K. (2007). Object-based classification of Ikonos imagery for mapping large-scale vegetation communities in urban areas. *Sensors*, 7, 2860-2880.

Matsuda, I. (2004). River morphology and channel processes. In e. b. Developed under the Auspices of the UNESCO, *Fresh Surface Water; Encyclopedia of Life Support Systems (EOLSS).* Oxford: EOLSS Publishers.

Melton, M. (1957). *An analysis of the relations among elements of climate, surface properties, and geomorphology.* New York: Dept. Geol.

Meybeck, M., Vörösmarty, C. J., Fekete, B. M., & Lammers, R. B. (2000). Geomorphometric attributes of the global system of rivers at 30-minute spatial resolution. *Journal of Hydrology*, 237, 17-39.

Milliman , J. D., & Syvitsk, J. P. (1992). *Geomorphic/Tectonic Control of Sediment Discharge to the Ocean: The Importance of Small Mountainous Rivers.* Chicago: University of Chicago Pres.

Minjie, C., Haixia, L., Su, W., Li, L., Zhang, C., & Yue, A. (2008). A comparison of Pixel-based and Object-oriented Classification Using SPOT5 Imagery. *WSEAS International Conference on Applied Mathematics.* Beijing.

Mishra, P., Singh, D., & Yamaguchi, Y. (2011). Land Cover Classification of PALSAR Images by Knowledge Based Decision Tree Classifier and Supervised Classifiers Based on SAR Observables. *Progress In Electromagnetics Research B,* Vol. 30, 47-70.

Myint, S. W., Gober, P., Brazel, A., Grossman-Clarke, S., & Weng, Q. (2011). Per-pixel vs. object-based classification of urban land cover extraction using high spatial resolution imagery. *Remote Sensing of Environment* , doi:10.1016/j.rse.2010.12.017.

NASA Astrounaut Photograph (2010). Image taken by Astronaut from the International Space Station. ftp://eol.jsc.nasa.gov/EFS_highres_ISS022_ISS022-E-19513.JPG via http://climate.nasa.gov/blogs/index.cfm?FuseAction=ShowBlog&NewsID=462.

Nageswara , R. K., Swarna, L. P., Hari , K. M., & Arun, K. P. (2010). Morphometric Analysis of Gostani River Basin in Andhra Pradesh State, India Using Spatial Information Technology. *International Journal Of Geomatics And Geosciences*, 1(2), 179-187.

Nuhu, M.-R. (2016). *Delineation and quantification of submerged aquatic vegetation (SAV) in inland lakes using multispectral sensors.* Enschede, The Netherlands: Unpublished.

Nyarko, B. K. (2007). *Floodplain wetland-river flow synergy in the White Volta River basin, Ghana.* Bonn: Dissertation.

Pal, M., & Mather, P. (2003). An assessment of the effectiveness of decision tree methods for land cover classification. *Remote Sensing of Environment*, 554-565.

Pal, M., & Mather, P. M. (2001). Decision Tree Based Classification of Remotely Sensed Data. *Centre for Remote Imaging, Sensing and Processing (CRISP), National University of Singapore; Singapore Institute of Surveyors and Valuers (SISV); Asian Association on Remote Sensing (AARS)* (pp. 5-9). Singapore: Paper presented at the 22nd Asian Conference on Remote Sensing.

Pisal, P. A., Yadav, A. S., & Chavan, A. B. (2013). Morphometric Analysis Of Bhogavati River Basin, Kolhapur District, Maharashtra, India. *IOSR*

Journal of Mechanical and Civil Engineering, Second International Conference on Emerging Trends in Engineering (SICETE) Dr. JJ Magdum College of Engineering, Jaysingpur , 1-8.

Pradhan, R., Ghose, M., & Jeyaram, A. (2010). Land Cover Classification of Remotely Sensed Satellite Data Using Bayesian and Hybrid Classifier. *International Journal of Computer Applications,* (0975-8887), 7, 1-4.

Queensland, G. (2015, October 14). *What causes bank erosion?* Retrieved from Queensland Government website: https://www.qld.gov.au/environment/land/soil/erosion/types/

Ramu, Mahalingam, B., & Jayashree, P. (2013). Morphometric analysis of Tungabhadra drainage basin in Karnataka using GIS. *Journal of engineering, computer & applied science*, vol 2, no.7.

Reineck, H. E., & Singh, I. B. (2012). Depositional sedimentary environments: with reference to terrigenous clastics. . *Springer Science & Business Media*.

Restrepo, J. D., & Kjerfve, B. (2000). The Pacific and Caribbean Rivers of Colombia: Water Discharge, Sediment Transport and Dissolved Loads. *The Journal of geology*, 108(1), 17-33.

Richardson, E. V., Simons, D. B., & Lagasse, P. F. (2001). *River Engineering for Highway Encroachments- Highways in the River Environment, Federal Highway Administration, Hydraulic Series No. 6,*. Washington, DC: Publication No. FHWA NHI 01-004.

Ripley, B. D. (2007). *Pattern recognition and neural networks.* . Cambridge university press.

Saha, K., Wells, N. A., & Munro-Stasiuk, M. (2011). An object-oriented approach to automated landform mapping: A case study of drumlins. *Computers & Geosciences*, 1324-1336.

Schumm, S. A. (1956). Evolution of Drainage Systems and Slopes in Badlands at Perth Amboy, New Jersey. *GSA Bulletin*, 597-646.

Selander, J. (2004). Influences on river morphology in a sediment-dominated system. *Chapter four*, 1-13.

Slingerland, R., & Smith, N. D. (1998). Necessary conditions for a meandering-river avulsion. *Geology*, 435-438.

Strahler, A. N. (1957). Quantitative analysis of watershed geomorphology. *Trans. Amer. Geophys. Union, 38* , 913-920.

Syed, S., Dare, P., & Jones, S. (2005). Automatic Classification of Land Cover Features with High Resolution Imagery and Lidar: An Object Oriented Approach. *Proceedings of SSC2005 Spatial Intelligence, Innovation and Praxis: The national biennial Conference of the Spatial Sciences Institute*, 512-522.

Thomas, A., & Ayuk, J. (2010). *Land use/land cover mapping of the Kuils-Eerste River catchment (Western Cape) through an integrated approach using remote sensing and GIS.* Application of satellite remote sensing to support water resources management in Africa: Results from the TIGER Initiative.

Tooke, T. R., Coops , N. C., Goodwin, N., & Voogt, J. (2009). Extracting urban vegetation characteristics using spectral mixture analysis and decision tree classification. *Remote Sensing of Environment*, 398-407.

UNEP, G. E. (2002). *Volta River Basin Transboundary Diagnostic Analysis.* Unpublished Technical Report.

Waikar, M. L., & Nilawar, A. P. (2014). Morphometric Analysis of a Drainage Basin Using Geographical Information System. *International Journal of Multidisciplinary and Current Research*, 179-184.

Walker, M. I., & Nilawar, A. P. (2014). Morphometric Analysis of a Drainage Basin Using Geographical Information System: A Case study. *International Journal of Multidisciplinary and Current Research*, 179-184.

Wang, L., Sousa, W. P., & Gong, P. (2004). Integration of object-based and pixel-based classification for mapping. *International Journal Remote Sensing*, 5655-5668.

Watts, J. D., & Lawrence, L. R. (2008). *Merging Random Forest Classification with an Object-Oriented Approach for Analysis of Agricultural Lands.* Beijing: The International Archives of the Photogrammetry, Remote Sensing and Spatial Information Sciences.

Wei, S., Minjie, C., Li, L., Zhang, C., Yue, A., & Li, H. (2008). A Comparison of Pixel-based and Object-oriented Classification Using SPOT5 Imagery. *Proceedings of the 13th WSEAS International Conference on APPLIED MATHEMATICS*, 321-326.

Weih, R. C., & Riggan, Jr., N. D. (2010). Object-Based Classification Vs. Pixel-Based Classification: Comparitive Importance of Multiresolution Imagery. *The International Archives of the Photogrammetry, Remote Sensing and Spatial Information Sciences, Vol. XXXVIII-4/C7*, 6.

Whipple, K. X. (2004). Bedrock rivers and the geomorphology of active orogens, Annual Review of Earth and Planetary Science. *doi:10.1146/annurev.earth.23.101802.120356*, 151-185.

Wohl, E., & Achyuthan, H. (2002). Substrate Influences on Incised-Channel Morphology. *The Journal of Geology, Vol. 110, No. 1* , 115-120.

WRC, W. R. (2008). *White Volta River Basin IWRM Plan.* Accra.

Yan, G. (2003). Pixel based and object oriented image analysis for coal fire research. *Enschede, Holanda*.

Zwet, J. V. (2012). *The creation of a reservoir in the White Volta River, Ghana: An analysis of the impact on river morphology.*